Challenge Journal of
CONCRETE RESEARCH LETTERS

Vol.8 No.4 (2017)

CFRP acidic environment acoustic emission compressive strength concrete corrosion cracking ductility durability ferrocement fly ash mechanical properties palm oil fuel ash reinforced concrete self-compacting concrete silica fume steel mesh strength strengthening superplasticizer water a[illegible]ion

ISSN 2548-0928

TULPAR ACADEMIC PUBLISHING

Challenge Journal of Concrete Research Letters

E-mail: *cjcrl@challengejournal.com*

Web page: *cjcrl.challengejournal.com*

TULPAR Academic Publishing
www.tulparpublishing.com

TULPAR ACADEMIC PUBLISHING

Challenge Journal of Concrete Research Letters

CONTENTS

TULPAR ACADEMIC PUBLISHING

Challenge Journal of Concrete Research Letters

Effect of aggregates with high gypsum content on the performance of concrete

Yousry B. I. Shaheen *, Fatma M. Eid, Eng Eman Mahmoud

Department of Civil Engineering, Menoufia University, Shebin ElKoum, Menofia, Egypt

ABSTRACT

Sulfates in fine aggregate are a major problem when it exists in excessive amount especially in the Middle East and Iraq. Most of sulfate salts in fine aggregate are composed of calcium, magnesium, potassium and sodium sulfates. Calcium sulfates is the most common salt present in fine aggregate. It is usually finding as gypsum. It is difficult to obtain the specific sulfates content in fine aggregate within standard specifications. This research was conducted to investigate the effect of adding different contents of gypsum to fine aggregate as a replacement by weight on some properties of two types of concrete {self-compacted concrete (SCC) and high strength concrete (HSC)}. In these work three bases mixes of each type of concrete are used: mixes with different contents of metakaolin, mixes with different contents of gypsum and mixes incorporating different contents of metakaolin and gypsum. This study is devoted to determine the allowable content of sulfates in fine aggregate. Three levels of gypsum were tested (0.5, 1, 1.5) % by weight of fine aggregate and three levels of metakaolin were tested (5, 10, 15) % by the weight of cement. The experimental program is devoted to produce concrete with different levels of metakaolin and gypsum and determine its mechanical properties such as compressive strength and splitting tensile strength. The results arrived from this work show that the optimum gypsum content was 1.5% by weight of fine aggregates for mixes of SCC which gives increases in compressive strength and tensile strength, and 1% gypsum for mixes of HSC, results showed also that the metakaolin improved the properties of the two types of concrete and increased the loss which caused by sulfates. The best mix ever in SCC is 1% gypsum with 5% metakaolin, and 1% gypsum with 10% metakaolin for HSC.

ARTICLE INFO

Article history:
Received 11 September 2017
Revised 3 December 2017
Accepted 26 December 2017

Keywords:
Gypsum
Internal sulfates
Metakaolin
Self-compacting concrete
High strength concrete

1. Introduction

Aggregates in Middle East contain high amounts of sulfates which considered a big problem. Most of sulfates in sand took the form of gypsum, which represents 95% of sulfates and the rest are sodium, magnesium, and potassium sulfates (National Center for Construction Laboratories of Iraq, 1981). Some international standers specify limits of SO_3 content in aggregates. For example, IQS 45 (Iraqi standard specification for aggregate, 1984) allows 0.5% and 1% of SO_3 in fine aggregates and coarse aggregates, respectively. In the complimentary British Standard to BS EN 206-1, it is reported that the maximum allowable SO_3 content in fine aggregate is 1%. However, due to the rareness of aggregates with low sulfate contents in Middle East, a lot of studies have been conducted to investigate the optimum content of sulfate in fine aggregates which improves properties of concrete and use of aggregate with SO_3 above the specified limits given by the international standards (Haider K. Ammash, 2013) investigated that the optimum gypsum content was 0.5% by weight of fine aggregates for all mixes which increases compressive strength by a range (5.9-10.1)% and in splitting tensile strength by a range (1.2-8.5)% for all mixes of self-compacting concrete with lime stone powder.

* *Corresponding author*. Tel.: +020-128-2643204 ; E-mail address: ybishaheen@yahoo.com (Y. B. I. Shaheen)
ISSN: 2548-0928 / DOI: https://doi.org/10.20528/cjcrl.2017.04.001

Al-Rawi, R.S and Abdul–Latif (1993) suggested a new test called "compatibility test" to investigate the possibility of using sands with relativity high SO_3 contents with suitable cement without deleterious effect on concrete. This work was carried out on seven cements, three ordinary cement, three sulfate resisting cement and white cement. The sand used had SO_3 contents between 0.18% and 1.5% and the mix is designed to give a compressive strength of 30MPA at 28 days. The results show that SO_3 contents in sand gives the maximum concrete strength which differs from one cement to other ranging from (0.18% to 1.5%) depending on the chemical composition and fitness of cement. Gesoglu et al. (2016) reported that the effect of gypsum did not have a significant effect on the compressive and splitting tensile strength of UHSC: however, there was a slight reduction in strengths at a largest gypsum content of 11.55%. Al-Rawi (1997) investigated the effect of the gypsum content of cement on several engineering properties of concrete cured by accelerated and normal methods. He stated that increased gypsum content results in a significant decrease in the slump of concrete and that there is an optimum gypsum content, considerably higher for accelerated cured concrete than for normally cured concrete, at which maximum strength is obtained. The optimum gypsum content under accelerate curing conditions may be used without risk of reduction in the durability of concrete caused by excessive, delayed expansion.

Alwash (2005) found the percentage in compressive strength of the mix with OPC and sand of zone 2 which contains sulfate of 1.5% by weight of it, compared with the reduction in strength of the mix with OPC and sand of zone 4 which contains sulfate of 1.5% by weight of it. At ages 7, 28 and 56 days the reduction was (30.86%-37.7%), (10.47%-17.9%) and (2.29%-8.16%) for air curing and (23.6%-28.4%), (7.7%-13.4%) and (5.8%-5.5%) for moist curing. The influence of sulfates on elastic modulus and indirect tensile strength was found to be somewhat likely to that influence on compressive strength.

Hussain (2008) investigated some mechanical properties of self-compacting concrete and effect of internal sulfates in fine aggregate on it with several filler types of such as powder of limestone, pigment and hydrated lime. The mechanical properties were flexural strength, modulus of elasticity, compressive strength, the ultrasonic pulse velocity, indirect tensile strength and schmidtrebound hammer tests. He found the optimum gypsum content at which the strength is maximum. Further increase in SO3 content beyond the optimum causes a decrease in strength and nondestructive tests. Dinakar (2012) This study presents the effect of incorporation metakaolin (MK) on the mechanical and durability properties of high strength concrete for a constant water/blinder ratio of 0.3. Four different mixtures (MK0, MK5, MK10, MK15) were employed to examine the influence of low water to binder ratio on concrete containing MK on the mechanical and durability properties. The control mixture (MK0) did not include MK. In mixtures (MK5 , MK10, and MK15) cement content was partially replaced with 5, 10, and 15% (MK) by mass, respectively . Trial mixture were conducted for target of strength and slump of 90 MPa and 100 25 mm. From the results, it was observed that 10% replacement level was the optimum level in terms of compressive strength. Beyond 10% replacement levels, the strength was decreased but remained higher than the control mixture. Compressive strength of 106 MPa was achieved at 10% replacement. Splitting tensile strength and elastic modulus value have also followed the same trend. In durability tests MK concretes have exhibited high resistance compared to control and the resistance increase as the MK percentage increases. This investigation reports that the local MK has the potential to produce high strength and high performance concrete.

The study of Alsallami (2016) aims to obtain the influence of adding Nano metakaolin on some mechanical properties of hardened concrete. She used three levels of SO_3 in sand .These levels were (0.27, 0.5 and 1% by weight of fine aggregate). One level of Nano metakaolin replacements (1% by weight of cement) were used in this work .The total of 6 NC mixtures were made, all based on the same control mixture. The mix proportions and w/c ratio kept constant for all mixes, the only variation in the mixture were the Nano metakaolin and SO_3 content in sand so as to investigate only the effect of sulfates on NC with various Nano metakaolin contents on its properties in hardened state and compared its behavior with the behavior of plain NC. The ratio of w/c was 0.5 to give slump 80 10%. Curing time was three ages (28, 60, 90) days. The experimental results show that there is an optimum gypsum content in sand (SO_3 = 0.5 % by weight of fine aggregates) which gives the highest results in compressive strength, splitting strength and modulus of elasticity of NC. As gypsum content increases beyond this limit, the above mechanical properties will be decreased.

2. Experimental Program

The research is devoted to enhancement of some properties of SCC and HSC with fine aggregate contains internal sulfates by a partial replacement of gypsum to fine aggregate by weight. This study is bifurcate of two types of concrete they are: first is effect of gypsum on performance of concrete and second is effect of incorporation of gypsum with metakaolin on performance of concrete. Three levels of gypsum content in fine aggregate were investigated; these levels were 0.5%, 1% and 1.5% by weight of sand. Three levels of metakaolin were investigated (5%, 10% and 15%) by weight of cement. In order to view the differences in behavior during the fresh state as well as the hardened state, some of tests were performed. The slump test, V-funnel and J-ring were performed on concrete in the fresh state. The tests for compressive strength, splitting tensile strength, flexural strength and modulus of elasticity were carried out on concrete specimens in the hardened state.

3. Materials

The materials used were obtained from local sources. These materials are described as follows:

Cement: Portland cement type I (CEMI42.5N), provided by the Suez Cement Co, meeting the requirement of E.S. 7417/2001, Table 1.

Fine aggregates: Natural siliceous sand from El-khatatba, Table 2.

Coarse aggregate: Dolomite size 10mm and 20mm.

Fly ash: Fly ashes complies with chemical and physical requirements of American specification (ASTM C618), Europe specification (EN450), Table 3.

Silica fume: Micro silica (silica fume) is by-product material resulting from industry of Ferro silicon alloys. The product is a rich silicon dioxide powder where the average particles size is around 0.1micrometers. Mechanical and physical properties are given in Table 4.

Gypsum: Gypsum is added to fine aggregate to obtain the required SO_3 content. The added gypsum is natural gypsum rock (brought from Sina factory). It was crushed and grounded to obtain nearly the same graduation of fine aggregate used in mix.

Metakaolin: Metakaolin is a pozzolanic material. It is obtained by calcination of kaolintic clay at a temperature between 500° C and 800° C, Table 5.

Super plasticizer: (1) Sikaviscocrete 3425 was used as viscosity enhancing agent (VEA). Its products to achieve the dual action effect of high-range water reducer and viscosity-modifying admixture, respectively. It meets the requirements for super plasticizers according to Swiss specification (SIA162(2989)), EUROPE specification (EN934-2), and American specification (ASTM-C-494) type G and F, Table 6. (2) Sikament 163M the second type of superplasticiser which used to provide the necessary workability for HSC. It complies with ASTM C494 type F, and B.S. 5057 part 3.

Water: Tap water without taste, smell, color, or turbidity was used for mixing and curing the cellular concrete product.

Table 1. Chemical component of OPC.

Constituents	Concentration in weight (%)
Silica as SiO_2	19.8
Alumina as AL_2O_3	5.6
Iron as Fe_2O_3	2.4
Potassium as K_2O	0.58
Calcium as Cao	65.9
Sodium as Na_2O	0.29
Sulphur as SO_3	2.8
Loss in ignition	1.2
Insoluble residue	0.4
Free lime	0.9
Lime saturation factor	100.4
Lime combination factor	98.9
Silica ratio	2.48
Alumina ratio	2.33
Tricalcium Silicate (C_3S)	65.1
Dicalcium Silicate (C_2S)	7.6
Tricalcium Aluminate (C_3A)	10.8
Tetracalcium Aluminate Ferrite (C_4AF)	7.3

Table 2. Sand gradation.

Sieve size (mm)	9.5	4.75	2.36	1.18	0.61	0.31	0.16
% passing	100	95-100	80-100	50-85	25-60	5-30	0-10
% passing used sand	100	100	94	80	50	15	0

Table 3. Typical chemical and physical properties of fly ash.

Physical properties	Value
Colour	Light gray
Specific gravity	2.2
Specific surface area	8m / gm
PH	1.2
Chemical analysis	Value
Silicon (SiO_2)	93.0
Aluminium (Al_2O_3)	34.0
Iron (Fe_2O_3)	3.5
Manganese (Mn_2O_3)	0.2
Calcium (CaO)	4.5
Magnesium (MgO)	1.5
Titanium (TiO_2)	0.6
Sulphur (SO_3)	0.3

Table 4. Typical chemical and physical properties of silica fume.

Typical chemical analysis		Physical properties		Particle size	
Silica SiO_2	53.5%	Relative density	2.2	Top cut, 90% passing	11 um
Aluminate AL_2O_3	34.3%	Theoretical surface area (cm^3/ gm)	13000	Top cut , 99% passing	25 um
Iron Fe_2O_3	3.6%	ph , in water	11-12		
Calcium CaO	4.4%	Moisture content	<0.2		
Potassium K_2O	0.8%	Color	Light grey		

Table 5. Typical chemical composition of metakaolin.

	Percentage of by mass
SiO_2	51.52
AL_2O_3	40.18
Fe_2O_3	1.23
CaO	2.0
MgO	0.12
K_2O	0.53
SO_3	0.0
TiO_2	2.27

Table 6. Typical properties of Viscocrete 3425.

Properties	Value
Appearance	Clear liquid
Density	1.08 kg/It (ASTM C494)
PH Value	4.0
Solid content	40% by weight
Chloride content	Zero

Table 7. Concrete mix design (high strength concrete 60 MPa).

Materials	Mixture proportion	Dry weight [Kg/m^3]
Standard type 10 Portland cement	1.00	500
Sand	0.86	430
Dolomite (10mm)	0.86	430
Dolomite (20mm)	1.718	859
Water	0.30	150[L/m^3]
Portland silica fume cement	0.15	75[Kg/m^3]

Table 8. Concrete mix design (self compacting concrete 40 MPa).

Materials	Content
Cement (Kg/m^3)	425
Fine aggregate (Kg/m^3)	686
Coarse aggregate (Kg/m^3)	838
Fly ash (Kg/m^3)	85
Water	148 [L/m^3]
Viscocrete	17 [L/m^3]

4. Preparation of Concrete Mixes

The required amount of gypsum was added to fine aggregate, in order to obtain the demand level of SO_3 in the sample then the fine aggregate and gypsum were mixed until a homogeneous mix is obtained. Metakaolin powder was mixed with the quantity of cement until the metakaolin particles were thoroughly dispersed between cement particles. Mixing procedure is important to obtain the required workability. Before starting to mix, it is necessary to keep the mixer clean, moist and free from previous mixes. The procedure used for mixing was as follows:

1- Adding the fine aggregate to the mixer with 1/3 water, and mixing for 1 minute.

2- Adding the powder (cement+filler) with another 1/3 mixing water, and mixing for 1 minute.

3- After that, the coarse aggregate is added with the last 1/3 mixing water and 1/3 of superplasticizer, and mixing for 1.5 minute then the mixture is left for 1.5 minute for rest. Then the remaining 2/3 of the superplasticizer is added and mixed for 1.5 minute.

The all experimental program as shown in Fig. 1.

4.1. Tests of fresh SCC

In this research, it is necessary to make fresh concrete tests. SCC is defined by its behavior when it is in fresh state. The slump flow, V-funnel, V-funnel at T5 and G-ring are all used for all mixes of SCC (Fatma El-Zhraa, 2007).

Slump flow test: The slump flow test is the most widely used method for evaluating concrete consistency and filling ability in the laboratory and at construction sites. The flowing ability of fresh concrete is described by slump flow investigated with a cone, Fig. 2.

V-Funnel and V-Funnel at T5 minutes tests: The V-funnel is used to measure the filling ability of SCC and can also be used to evaluate the material segregation resistance, Fig. 3.

J-Ring test: The J-ring test is used to assess the passing ability of self-compacting concrete to flow through tight opening including spaces between reinforcing bars, Fig. 4.

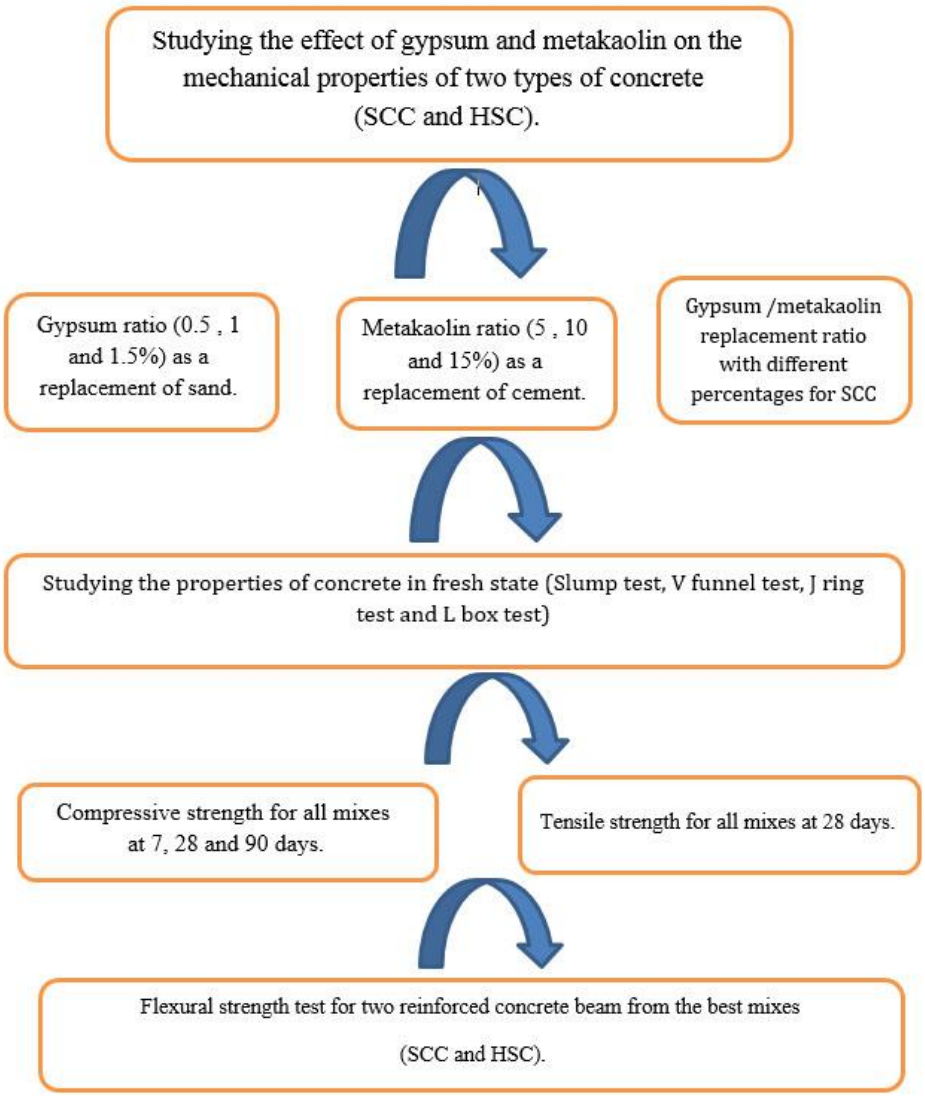

Fig. 1. Reinforcement details of all slabs.

Fig. 2. Slump test.

Fig. 3. J.Ring test.

Fig. 4. V-funnel test.

4.2. Tests of hardened concrete

Compressive strength: The compressive strength was conducted on cubes(15x15x15cm) at ages of (7, 28 and 90 days) by using a hydraulic compression machine with a capacity of 2000 KN. The average of three test cubes was adopted for each mix, Fig. 5.

Splitting tensile strength: This test was conducted on cylindrical concrete specimens (100x200 mm) after 28 days. Each splitting tensile strength value was the average of two specimens.

Fig. 5. Slump test.

5. Results and Discussion

5.1. SCC

5.1.1. Compressive strength

The compressive strength test results of concrete specimens were tested at ages (7, 28 and 90 days), three cubes are tested at each age. Compressive strength of SCC with various percentages of gypsum and metakaolin are shown in Table 9 and Fig. 10.

It can be seen that for all mixes, there as an optimum SO_3 content at which the compressive strength is maximum. The present data indicates that the optimum SO_3 content for these mixes is about (1.5%) by weight of sand Fig. 7.

From the results of compressive strength, it can be noticed that:

1- When gypsum content in fine aggregate increase to 0.5%, this leads to a decrease in compressive strength in the range (3.23 and 2.28)% at ages (7 and 28)days respectively and an increase at age of 90 days by 8.75%.

2- When gypsum content increase from (0.5 to 1)% , this leads to an increase in compressive strength in the range (2.27 and 0.88)% at ages (7 and 28) respectively and a slight reduction at age of 90 days by 0.94%.

3- When gypsum content in fine aggregate increases to 1.5% , this leads to an increase in compressive strength in the range (6.4, 17 and 7.8)% at ages (7,28 and 90) days respectively.

Also, results showed that the use of metakaolin(MK) improved the compressive strength of concrete for all sulfates content and for all ages as shown below (Fig. 8):

1- When MK added to cement by 10% without gypsum in fine aggregate, this leads to an increase in compressive strength in the range (4.5 , 12.8 and 14.7) at ages (7, 28 and 90) days respectively.

2- When MK added to cement by (5, 10 and 15)% for the mix of 0.5 % gypsum, the best level of MK was 15 % which leads to an increase in compressive strength in the range (2.8, 11.45 and 5.6) at ages (7, 28 and 90) days respectively.

3- When MK added to cement by (5, 10 and 15)% for the mix of 1% gypsum, the best level of MK was 5% which leads to an increase in compressive strength in the

range (9.5, 13.2 and 21.6) at ages (7, 28 and 90) days respectively.

4- When MK added to cement by (5, 10 and 15)% for the mix of 1.5% gypsum, the best level of MK was 5% which leads to an increase in compressive strength in the range (0.6 and 5.8) at ages (28 and 90) days respectively.

The results indicated that the MK improved the properties the mixes of SCC and increase the compressive strength for the mixes with gypsum.

5.1.2. Splitting tensile strength

Results of splitting tensile strength at 28 days of SCC with various percentages of gypsum and MK are presented in Table 9. It is clear that the effect of sulfates on the splitting tensile strength is somewhat similar to that on compressive strength. For all mixes, there is an optimum SO_3 % which splitting tensile strength is maximum (Fig. 11). The present data indicates that the optimum SO_3 content for these mixes is about (1.5%) by weight of sand. From the results in Table 9, it can be noticed that:

1- When SO_3 in fine aggregate increase to 0.5% , this leads to decrease in splitting tensile strength of the concrete by (21.8)% at age of 28 days.

2- When SO_3 in fine aggregate increase to 1%, this leads to decrease in splitting tensile strength of concrete by (31.25)% at age of 28 days.

3- When SO_3 in fine aggregate increase to 1.5%, this leads to an increase in splitting tensile strength by (6.25)% at age of 28 days.

In addition also, results showed that the use of 5% MK in SCC was the best compared with the mixes that contain gypsum only by improving splitting tensile strength loss for all sulfates content as shown below (Fig. 8):

1- When MK added to cement by 5% to the mix of 0.5% gypsum, this leads to an increase in splitting tensile strength by 12% at age of 28 days.

2- When MK added to cement by 5% to the mix of 1% gypsum, this leads to an increase in splitting tensile strength by 18% at age of 28 days.

3- When MK added to cement by 5% to the mix of 1.5% gypsum, this leads to decrease in splitting tensile strength by 11.7% at age of 28 days.

Table 9. Results of mixes of SCC.

MIX	GYPSUM	MK	Compressive strength (kg/cm²)			Tensile strength (kg/cm²)
			7 days	28 days	90 days	28 days
C1	0%	0%	430	570	650	43
C2	0%	5%	453	588.9	704	54
C3	0%	10%	449.4	643.2	745.5	38.2
C4	0%	15%	452.3	543.6	653.2	36.6
C5	0.5%	0%	416.1	557	708.8	33.4
C6	1%	0%	439.2	575	643.9	28.6
C7	1.5%	0%	457.5	667	702	46.2
C8	0.5%	5%	422.4	562.7	643.4	47.8
C9	0.5%	10%	439.5	594.2	672.5	38.2
C10	0.5%	15%	442.1	635	686.4	31.8
C11	1%	5%	470.9	645.2	790.4	51
C12	1%	10%	458.5	610.4	732.5	44.6
C13	1%	15%	460.3	556.6	667.9	39.2
C14	1.5%	5%	473.3	573.4	687.7	38.2
C15	1.5%	10%	449.8	539.7	647.8	41.4
C16	1.5%	15%	4565	547.5	656.9	46.2

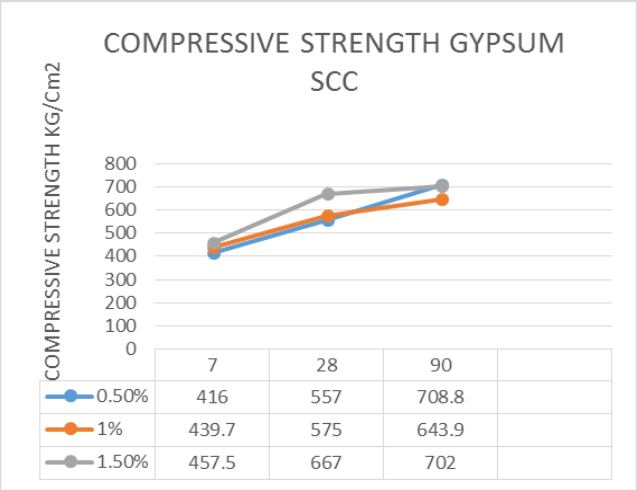

Fig. 6. Compressive strength for gypsum mixes of SCC.

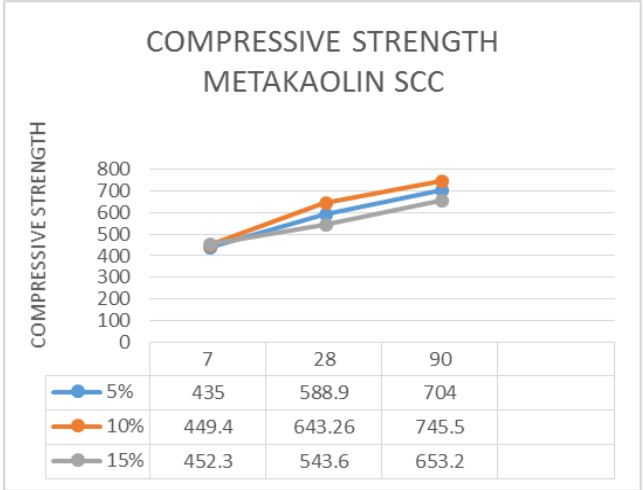

Fig. 7. Compressive strength for MK mixes of SCC.

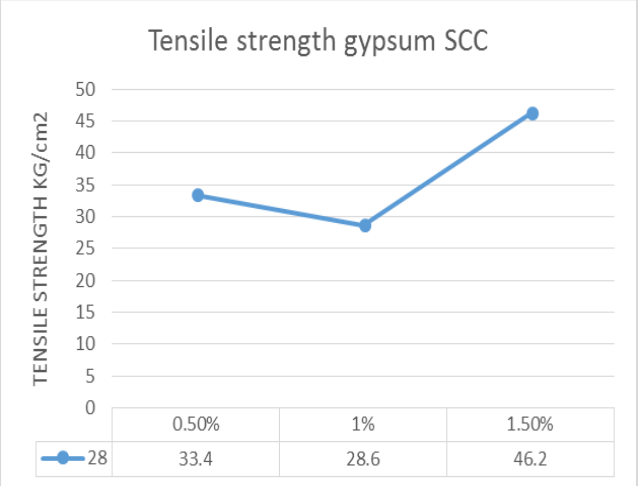

Fig. 8. Tensile strength for gypsum mixes of SCC.

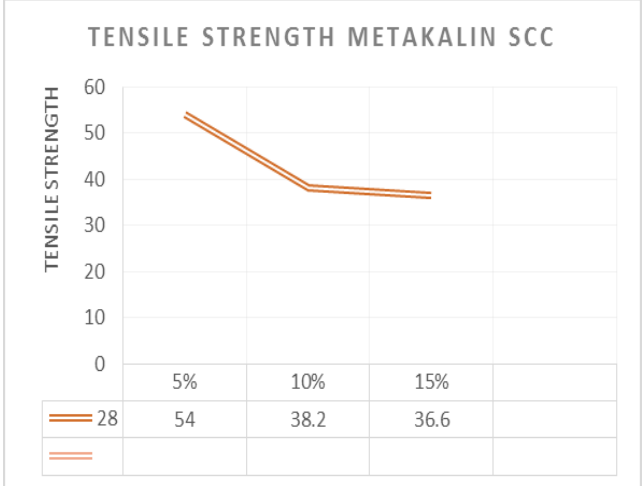

Fig. 9. Tensile strength for MK mixes of SCC.

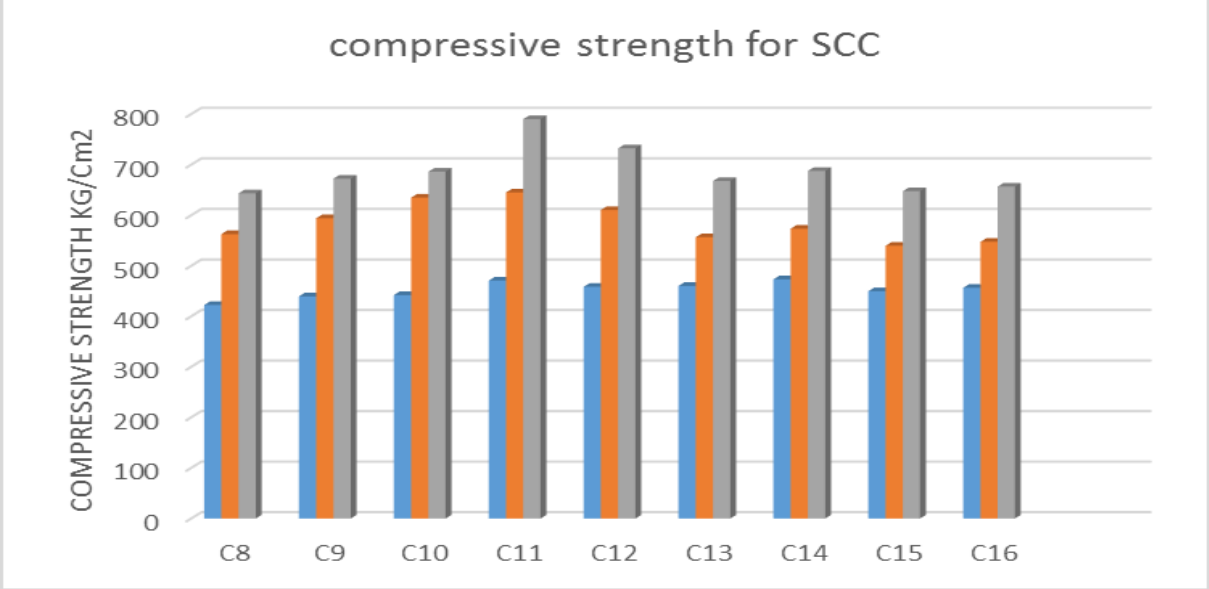

Fig. 10. Compressive strength for mixes of SCC.

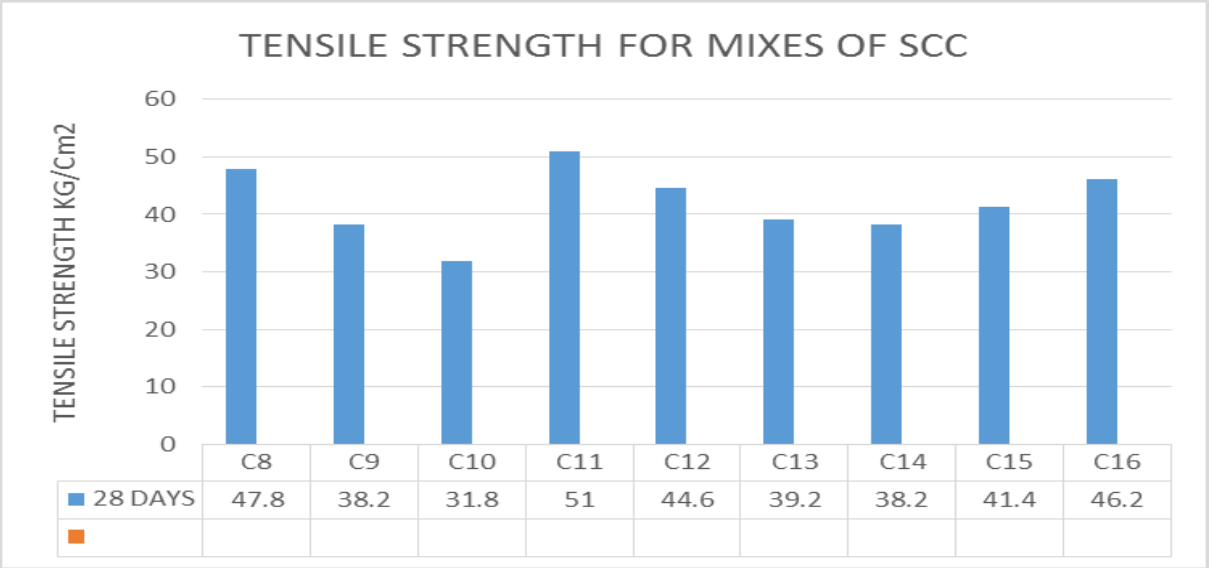

Fig. 11. Tensile strength for mixes of SCC.

5.2. HSC

5.2.1. Compressive strength

The compressive strength test results of the concrete specimens were tested at ages (7, 28 and 90 days), three cubes are tested at each age. Compressive strength of HSC with various percentages of gypsum and metakaolin are shown in **Table 10 and Fig. 16.**

It can be seen that for all mixes, there as an optimum SO_3 content at which the compressive strength is maximum. The present data indicates that the optimum SO_3 content for these mixes is about (1.5%) by weight of sand **(Fig.12).**

From the results of compressive strength, it can be noticed that:

When gypsum content in fine aggregate increase to 0.5%, this leads to a increase in compressive strength in the range (9.5, 11.48 and 14)% at ages (7 , 28 and 90) days respectively

2- When gypsum content increase from (0.5 to 1)% , this leads to an increase in compressive strength in the range (17.5 ,20.3 and 25.33)% at ages (7 , 28 and 90) days respectively.

3- When gypsum content in fine aggregate increases to 1.5%, this leads to an increase in compressive strength in the range (26.4, 30.7 and 36.4)% at ages (7,28 and 90) days respectively.

Also results of use metakaolin improved the compressive strength of concrete for all sulfates mixes as shown below **(Fig. 13):**

1- When MK added to cement by 10% without gypsum in fine aggregate, this leads to an increase in compressive strength in the range (10.5 , 21.3 and 25.4) at ages (7, 28 and 90) days respectively.

2- When MK added to cement by (5, 10 and 15)% for the mix of 0.5 % gypsum, the best level of MK was 10 % which leads to an increase in compressive strength in the range (14.6, 22.5 and 60) at ages (7, 28 and 90) days respectively.

3- When MK added to cement by (5, 10 and 15)% for the mix of 1% gypsum, the best level of MK was 5% which leads to an increase in compressive strength in the range (13.4, 28.4 and 55) at ages (7, 28 and 90) days respectively.

4- When MK added to cement by (5, 10 and 15)% for the mix of 1.5% gypsum, the best level of MK was 5% which leads to an increase in compressive strength in the range (6.8, 14.6 and 18.7) at ages (7, 28 and 90) days respectively. The results indicated that the MK improved the properties the mixes of HSC and increase the compressive strength for the mixes with gypsum.

5.2.2. Splitting tensile strength

Results of splitting tensile strength at 28 days of HSC with various percentages of gypsum and MK are presented in **Table10** and **Fig. 17**. It is clear that there is an optimum SO_3 % which splitting tensile strength maximum. The present data indicates that the optimum SO_3 content for these mixes is about (1%) by weight of sand. From the results in **Table 10** and F**ig. 14** it can be noticed that:

1- When SO_3 in fine aggregate increase to 0.5% , this haven't any changes in splitting tensile strength of the concrete at age of 28 days.

2- When SO_3 in fine aggregate increase to 1%, this leads to increase in splitting tensile strength of concrete by (38.8)% at age of 28 days.

3-When SO_3 in fine aggregate increase to 1.5%, this leads to an increase in splitting tensile strength by (33.3)% at age of 28 days.

Also, results showed that the use of 10% metakaolin (MK) improved the tensile strength of concrete for all mixes which contain MK only without gypsum **Fig. 15,** and the use of 10% MK in HSC was the best compared with the mixes that contain gypsum only by improving splitting tensile strength loss for all sulfates content as shown below:

1- When MK added to cement by 10% to the mix of 0.5% gypsum, this leads to an increase in splitting tensile strength by 55.5% at age of 28 days.

2- When MK added to cement by 10% to the mix of 1% gypsum, this leads to an increase in splitting tensile strength by 66.6% at age of 28 days.

3- When MK added to cement by % to the mix of 1.5% gypsum, this leads to increase in splitting tensile strength by 60.2 at the age of 28 days.

Table 10. Results of mixes of SCC.

MIX	GYPSUM	MK	Compressive strength (kg/cm²)			Tensile strength (kg/cm²)
			7 days	28 days	90 days	28 days
H1	0%	0	490.2	603.3	724.4	28.7
H2	0%	5%	544.4	653.3	790.5	35
H3	0%	10%	418.9	515.3	618.4	39.8
H4	0%	15%	576.1	720.2	864.3	33.4
H5	0.5%	0%	556.8	668.2	801.8	28.7
H6	1%	0%	570.2	724.8	871.5	39.8
H7	1.5%	0%	654.3	799.5	900.4	38.2
H8	0.5%	5%	558.7	670.4	905	42.9
H9	0.5%	10%	585.2	702.2	906	44.6
H10	0.5%	15%	551.1	661.4	793.6	35
H11	1%	5%	670.2	804.1	900	42
H12	1%	10%	622.9	747.5	897.1	47.8
H13	1%	15%	566.3	679.5	815.4	33.7
H14	1.5%	5%	601.6	751.98	903.4	42.6
H15	1.5%	10%	504.3	722.4	867.5	47
H16	1.5%	15%	570.6	684.7	823.4	35.7

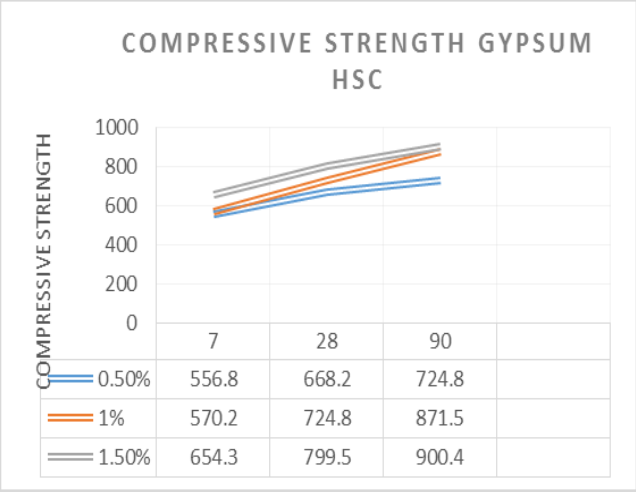

Fig. 12. Compressive strength of gypsum mixes for HSC.

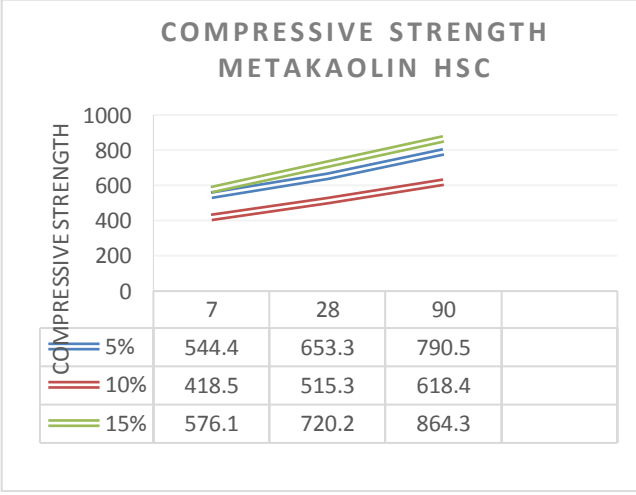

Fig. 13. Compressive strength of MK mixes for HSC.

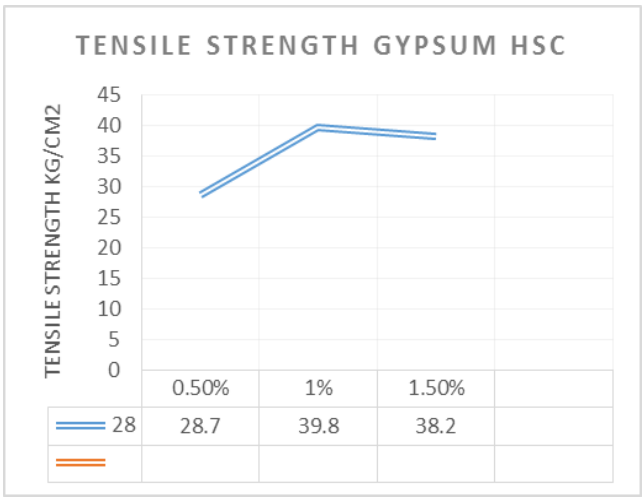

Fig. 14. Tensile strength of gypsum mixes of HSC.

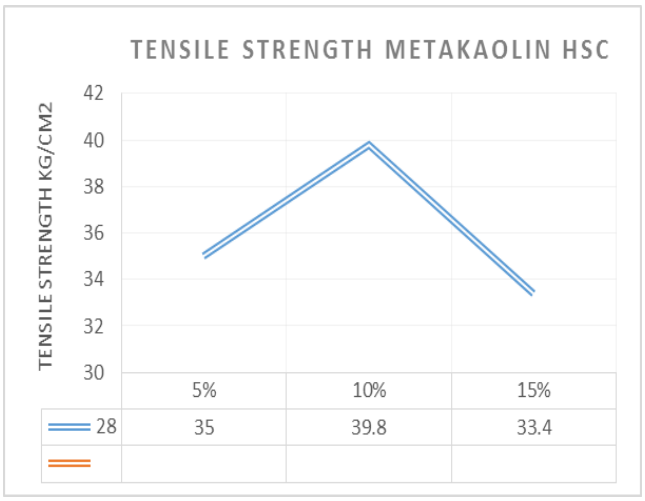

Fig. 15. Tensile strength of MK mixes of HSC.

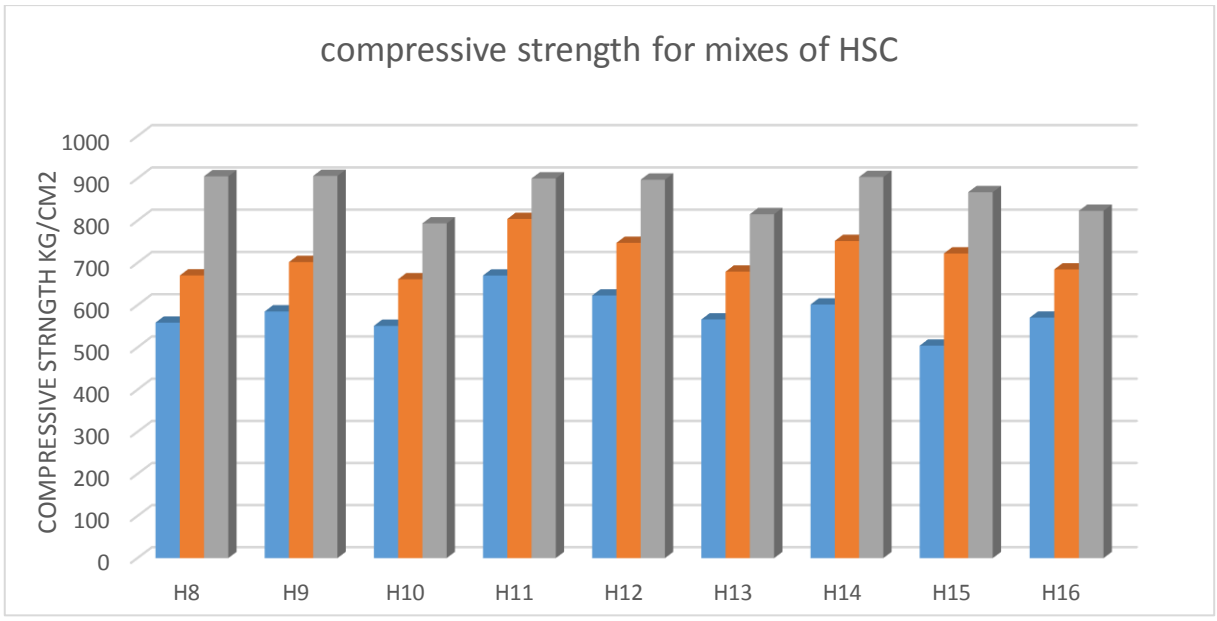

Fig. 16. Compressive strength for mixes of HSC.

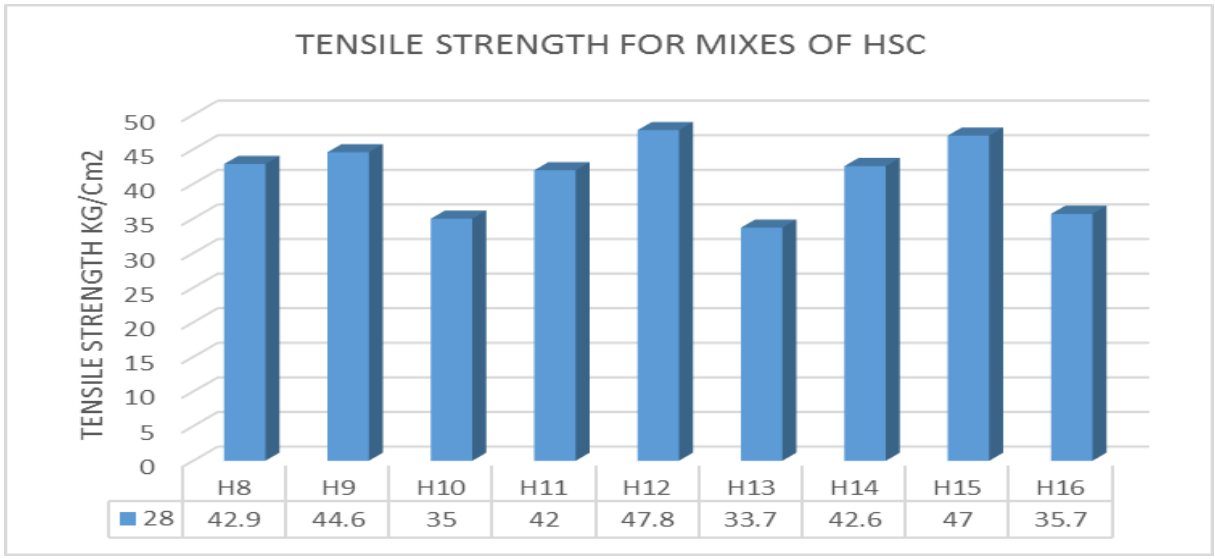

Fig. 17. Tensile strength for mixes of HSC.

5.3. Results of flexural test of beams

Two reinforced concrete beams were cast and tested (one cast with HSC using mix No.(H15) and another with SCC using mix No.(C16)) ,with cross section of 15*20 cm and a total length 100 cm, and tested under four lines loadings with span 90 cm until failure. The two beams reinforced with 2 Φ12mm at the bottom, and 2 Φ8mm at the top in and number of stirrups 5 Φ6mm/m.

The two beams were test after 28 days of curing; the beams were tested with using ELE calibrated flexural testing machine of capacity 100 KN. During testing process deflections and tensile and compressive strains were measured by using dial gauges and mechanical strain gages. Cracking patterns were detected with their loadings. And ultimate loads were recorded at each load increment; four readings were recorded for strain, and deflection .The test devices and arrangements shown in Fig. (21).

Results indicated that the beams of best mixes are a stiff beams which carried a maximum load of 65.20 KN (of SCC) mix and 79.40 KN of (HSC mix). Fig 19. It is interesting to note from Fig. 19 that the first crack loads of beam SCC and beam HSC were 30 and 40 KN respectively while the serviceability loads of beam SCC and beam HSC were reached 54 and 62KN respectively. The ductility ratio of beam SCC and beam HSC achieved 54, 62 KN respectively while the calculated energy absorption of beams SCC and HSC arrived 211.33 and 323,58 KN.mm respectively, therefore there is increase in first crack loads, serviceability loads, ductility ratio for HSC beams compared with those of SCC beams.

Fig. 18. ELE flexural 100KN testing machine.

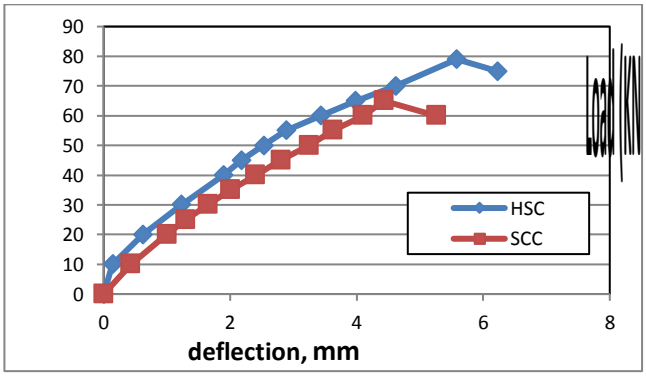

Fig. 19. load deflection curve for beams (HSC, and SCC).

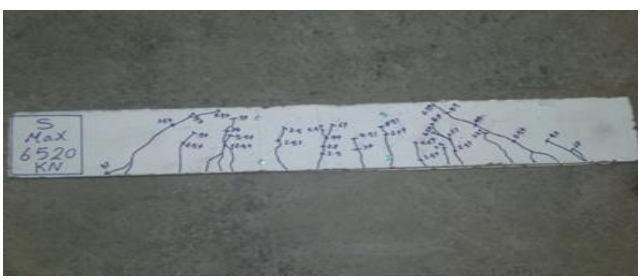

Fig. 22. Crack Pattern of beam SCC.

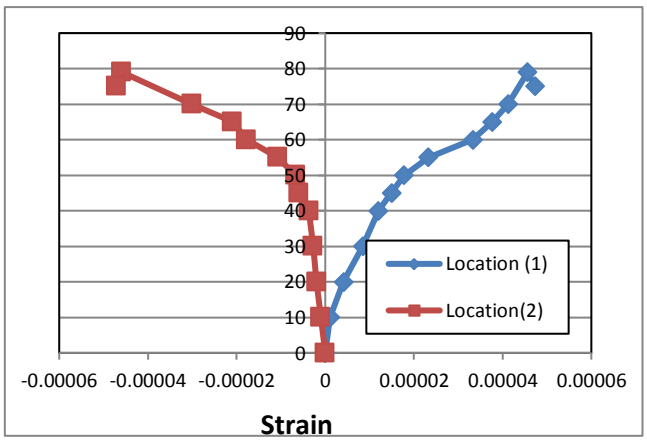

Fig. 20. Concrete strains curves for HSC beam.

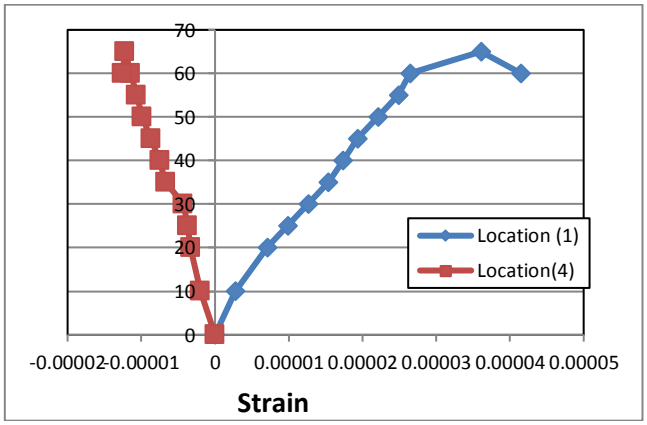

Fig. 21. Concrete strains curves for SCC beam.

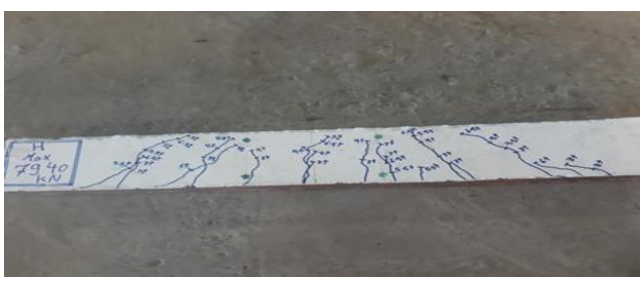

Fig. 23. Crack Pattern of beam HSC.

6. Conclusions

6.1. SCC

- Mixes with gypsum content in fine aggregate as a replacement by 1.5% are the best content which played actual role to improve both compressive and tensile strengths.
- Mixes with metakaolin 10% and 5% replacement of cement increase compressive strength and indirect tensile strength respectively.
- Mix with 1% gypsum and 5% metakaolin was found to be the best mix which increased the compressive strength at ages 7, 28 and 90 days and increased indirect tensile strength in 18% at 28 days age.

6.2. HSC

- Mixes with gypsum content in fine aggregate as a replacement by 1.5 % are the best which increase the compressive strength at all ages of 7,28 and 90 days and 1% gypsum content for indirect tensile strength at all age 28 days.
- The best content of MK for mixes without gypsum is 10% as a replacement of cement.
- Mixes with 5% MK and 1% gypsum is the best mix which increase the compressive strength at all ages, and the mix of 0.5% gypsum with 5% and 10% MK are the best mixes which improve the compressive strength at age 90 days.
- Mixes with 1% gypsum and 10% MK improve indirect tensile strength at age 28 days.
- Tested beams SCC and HSC emphasized high ductility and energy absorption properties which are very useful for dynamic applications. The energy absorption of beam HSC is1.53 times that of beam SCC.
- There is no spalling of concrete cover of the tested beams at failure, this is predominant.
- The developed cracks at failure were fine crack widths resulting from employing the proper designed mix.

REFERENCES

Al-Rawi RS (1997). Gypsum content of cements used in concrete cured by accelerated methods. *Journal of Testing and Evaluation*, 5(3), 231-236.

Al-Rawi RS, Abdul–Latif AM (1998). Compatibility of sulphate contents in concrete ingredients. *Fourth Scientific Conference*, College of Engineering of Baghdad University.

Alsallami ZHA (2016). Effect of sulfate in sand on some mechanical properties of nano metakaolin normal concrete. Journal of Babylon University/Engineering Sciences, 24(1), 107-116.

Alwash JJ (2005). Effect of Sulfates in Fine Aggregate on drying Shrinkage Cracking in End Restrained Concrete Members. *M.Sc. Thesis*, University of Babylon, College Of Engineering.

Ammash HK, AL-Baghdadi HM, AL-Salim NHA (2013). Effect of Sulfates in Fine Aggregate on Some Properties of Self Compacting Concrete Incorporating High Reactive Metakaolin. AL-Qadisiyia University, Iraq, Babylon University.

BS 8500-2 (2005). Concrete, complementary British standard to BS EN 206-1, specification for constituent materials and concrete, British Standard Institution.

Dinakar P, Sahoo PK, Sriram G (2013). Effect of metakaolin content on the properties of high strength concrete. *International Journal of Concrete Structures and Materials*, 7(3), 215–223.

Emborg M (2000). Mixing and Transport. Brite EuRam, Task 8.1.

Fatma El-Zhraa (2007). Behavior of Reinforcement Concrete Elements Strengthened with Fiber Reinforced Polymers Under Different Loading Conditions. Chapter 2. Menoufiya University.

Gesoglu M, Güneyisi E, Nahhab AH, Yazıcı H (2016). The effect of aggregates with high gypsum content on the performance of ultra-high strength concretes and Portland cement mortars. *Construction and Building Materials*, 110, 346-354.

Hussain TH (2008). Effect of Sulfates in Fine Aggregate on some Mechanical Properties of Self Compacting Concrete. *M.Sc. Thesis*, University of Babylon, College Of Engineering.

IQS 45 (1984). Iraqi standard specification for aggregate from natural sources for concrete and building construction. ICOSQC, Baghdad, Iraq.

National Center for Construction Laboratories of Iraq (1981). Suggestion for the determination of sulfate content in sand. In Arabic.

Challenge Journal of Concrete Research Letters

Seismic fragility curves for mid-rise reinforced concrete framed structures with different lateral loads resisting systems

Ghada Mousa Hekal [a], Kamel Kandeel [a,*], Mostafa Morsi El-Shami [b], Ahmed Dawod [a]

[a] *Department of Civil Engineering, Menoufia University, Shebin ElKoum, Menofia, Egypt*
[b] *Department of Construction Engineering, University of Dammam, Dammam 34212, Saudi Arabia*

ABSTRACT

The current study presents lateral load analysis of mid-rise reinforced concrete framed structures with two different lateral load resisting systems; shear walls and rigid marginal beams. The main objective here is to investigate the influence of the location of the system in the structure; i.e. arrangement of shear walls and level of the marginal beam. For that purpose, seismic fragility curves are used as an assessment tool for comparing the seismic performance of the studied structures in different situations. Incremental dynamic analysis was performed under ten ground motions to determine the yielding and collapse capacity of each building. Five performance levels were considered in the analysis. These performance levels are (i) operational, (ii) immediate occupancy, (iii) damage control, (iv) life safety and (v) collapse prevention. Fragility curves were developed for the structural models of the studied structures considering the previously mentioned performance levels. It was observed that arrangement of shear walls on the long direction of the structure has insignificant effects on its performance while interior shear walls provide the best behavior of the structure compared to exterior shear walls only and distributing shear walls internally and externally. The analysis outcomes also indicated that the presence of the rigid marginal beam in the lower storey gives more efficiency regarding to lateral loads resistance in the studied structure.

ARTICLE INFO

Article history:
Received 2 October 2017
Accepted 15 November 2017

Keywords:
Seismic fragility curves
Incremental dynamic analysis
Shear wall position
Rigid marginal beam level
Performance-based design
Seismic risk analysis

1. Introduction

Shear walls and rigid marginal beams are the most common tools used for resisting lateral loads in mid-rise structures. However, the arrangement of shear walls and the levels of rigid marginal beam in the building affect the structure performance. Talaeitaba et al. (2014) found that the value of response modification factor, in comparison with the presented value in ASCE7 code, was varied between -18% to +25% over changing the arrangement of the shear walls.

Earthquakes may cause extensive losses. Among which, structural damage plays an important role. One of the most important tools in evaluating the seismic damage to structures is the fragility curves. The fragility curves for certain type of building structure are used to represent the probabilities that the structural damages, under various levels of seismic excitation, exceed specified damage level. In other words, each point on the curve represents the probability that the spectral displacement under certain level of ground shaking is larger than the displacement associated with certain damage state (Cherng, 2001).

Performance-based design aims to satisfying owners and users of structures by selecting the desired performance level of the structure under different earthquakes (SEAOC, 1995; Hamburger, 1998; Federal Emergency Management Agency (FEMA) 349, FEMA/EERI, 2000; ATC, 2002; Vamvatsikos and Cornell, 2002). The desired performance level affects design and construction costs. The performance level is an expression of the maximum desired extent of damage to a structure under specific earthquake design level.

* *Corresponding author*. Tel.: +20-106-985-6009 ; E-mail address: gahda.mousa@sh-eng.menofia.edu.eg (G. M. Hekal)
ISSN: 2548-0928 / DOI: https://doi.org/10.20528/cjcrl.2017.04.002

The overall building performance is categorized by FEMA 273 (1997) / 356 (2000) in terms of both the structural and non-structural performance levels as Operational, Immediate Occupancy, Life Safety and Collapse Prevention.

Incremental dynamic analysis, IDA, is a parametric analysis method used to estimate structural performance under seismic loads. During IDA, The structural model is subjected to several ground motion records, each scaled to multiple levels of intensity, and thus producing response curves parameterized versus intensity levels. IDA gives a clear vision about the performance of a certain type of structures under seismic excitations with wide range of intensities (Vamvatsikos and Cornell, 2002).

Many researchers developed and used IDA curves in their research. Uriz and Mahin (2004) used IDA to study seismic performance of concentrically braced steel frames. Kircil and Polat (2006) developed IDA curves for mid-rise RC frames in Istanbul. Mander et al. (2007) developed IDA curves for bridge structures and then the IDA results were integrated into a probabilistic risk analysis procedure. Ibrahim (2009) performed IDA on typical moment-resisting frames located in Egypt. Ibrahim and El-Shami (2011) carried out IDA for four and eight-storey multistorey reinforced concrete (RC) frame buildings in Saudi Arabia. Moridani and Khodayari (2013) studied the influence of different seismic sources characteristics on the outcomes of IDA.

Farsi et al. (2015) presented a work to estimate the seismic vulnerability of existing buildings in Algeria. Raipure (2015) presented a study on development of fragility curves for open ground storey buildings. She used probabilistic seismic demand model (PSDM) as per power law for the generation of fragility curves. Vazurkarand Chaudhari (2016) discussed HAZUS methodology for the generation of fragility curves and the fragility curves are generated for low-rise RC building structures without considering infill walls. Rehman and Cho (2016) produced probability damage maps for four damage levels and three structure types.

The inter-storey drift ratio, i.e. the ratio of storey drift between two consecutive floors to storey height, is considered as a significant cause that leads to the damage of building structures when subjected to earthquake ground motion. Hence, performance levels are usually expressed in terms of inter-storey drift ratios i.e. storey drift divided by storey height. FEMA 356 provided typical values of inter-storey drift ratios for different structural systems for various structural performance levels. For concrete frames, the values are 1%, 2% and 4% for immediate occupancy (IO), life safety (LS) and collapse prevention (CP), levels, respectively. Based on many references

Xue et al. (2008) suggested values of maximum inter-storey drift ratio for each performance level for different structural systems. For systems rather than that with masonry shear walls, the values of maximum inter-storey drift ratios for performance levels; operational (OP), immediate occupancy (IO), damage control (DC), life safety (LS) and collapse prevention (CP) are tabulated in Table 1.

Table 1. Maximum inter-storey drift ratios for different performance levels (Xue et al. 2008).

Performance level	OP	IO	DC	LS	CP
Maximum inter-storey drift ratio	0.005	0.010	0.015	0.02	0.025

2. Structural Models

Two reinforced concrete framed structures were selected for analysis in this research.

The first structure is one bay-eight storey space frame with 3m storey height and 4m bay width. The frames are 5m apart. Dimensions of this structure were selected so that it has a strong direction and a weak direction. In the analysis, the structure was subjected to earthquakes in the strong direction as CASE 1-1 and in the weak direction as CASE 1-2. To understand the behavior of the structure in the two studied cases, all shear walls were arranged to resist the ground motion in each case. So, four different structural systems were studied for each case. The investigated structures are described according to arrangement of shear walls as follows:

CASE 1-1
SW1: Frame without shear walls,
SW2: Frame with exterior shear walls,
SW3: Frame with interior shear walls, and
SW4: Frame with exterior and interior shear walls

CASE 1-2
SW5: Frame without shear walls,
SW6: Frame with exterior shear walls,
SW7: Frame with interior shear walls, and
SW8: Frame with exterior and interior shear walls

The second structure is a symmetric two bays-six storey space frame with 3m storey height, 4m bay width and frames are 4m apart. Six different structural systems were studied for this frame as CASE 2-0 depending on the level of the rigid marginal beam in the structure.

CASE 2-0
MB1: Structure without rigid marginal beam,
MB2: 1st storey with rigid marginal beam,
MB3: Lower storey with rigid marginal beam,
MB4: Medium storey with rigid marginal beam,
MB5: Upper storey with rigid marginal beam, and
MB6: All floors with rigid marginal beams.

The structure models are shown in Figs. 1, 2 and 3, while Table 2 shows the cross sections and reinforcement of beams, columns and shear walls.

All structures were designed according to the Egyptian Code of practice (No. 203, 2007) with compressive strength of concrete 250 kg/cm^2 and yielding stress of reinforcing steel 3600 kg/cm2. The soil condition was selected as soil class C, which is medium soil. The structures were classified as low hazard buildings, with importance factor I = 1. Design ground acceleration of 0.125g was considered as the structures were assumed to be in Alexandria (Zone 2).

Table 2. Cross sections of beams, columns and walls.

Model	Beam			Column	Wall
Maximum inter-storey drift ratio	B	B1	B2	C	W
Dimensions, cm	20×60	20×50	20×70	40×40	30×200
Reinforcement, mm	12Φ16	8Φ16	12Φ16	16Φ12	50Φ12

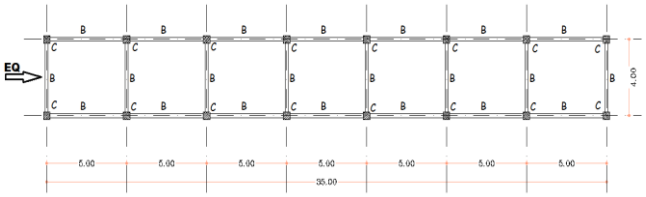

SW1, Natural Period 'T'= 0.97162519 sec

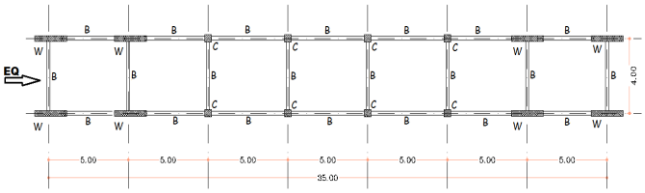

SW2, Natural Period 'T'= 1.05706765 sec

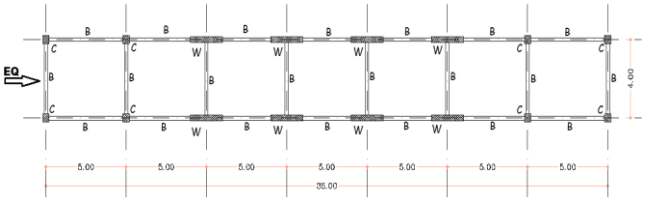

SW3, Natural Period 'T'= 1.0570553 sec

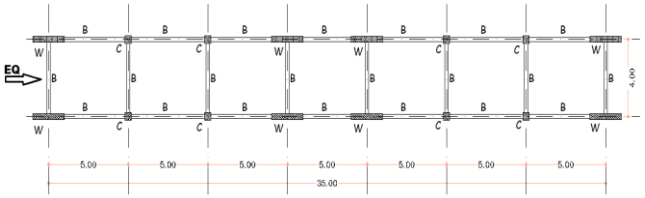

SW4, Natural Period 'T'= 1.05595999 sec

Fig. 1. Structural models for CASE 1-1 (plan views).

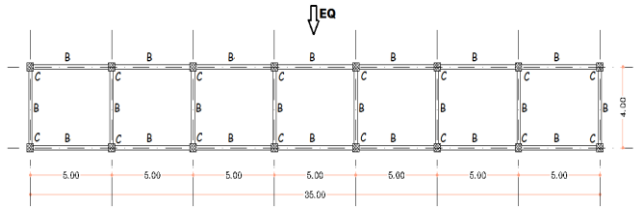

SW5, Natural Period 'T'= 0.97162519 sec

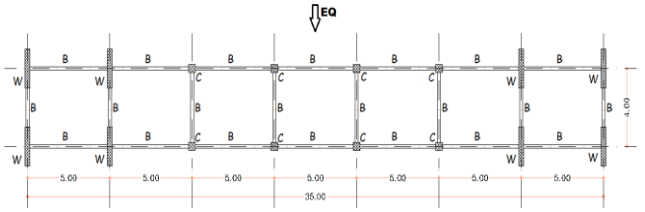

SW6, Natural Period 'T'= 0.92561894 sec

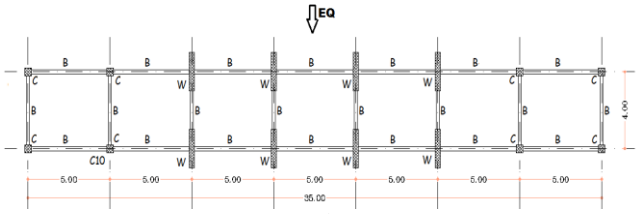

SW7, Natural Period 'T'= 0.90634853 sec

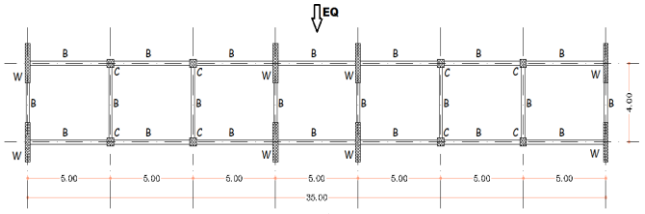

SW8, Natural Period 'T'= 0.93025108 sec

Fig. 2. Structural models for CASE 1-2 (plan views).

During the IDA using SeismoStruct, the concrete was modeled using a uniaxial constant confinement concrete model initially presented by Madas (1993). The confinement effects provided by the lateral transverse reinforcement are included through the model introduced by Mander et al. (1988) which assumed constant confining pressure throughout the entire stress–strain range. The reinforcing bars were modeled using a uniaxial bilinear stress-strain model with kinematic strain hardening.

The elastic range remains constant throughout the various loading stages, and the kinematic hardening rule for the yield surface is assumed as a linear function of the increment of plastic strain.

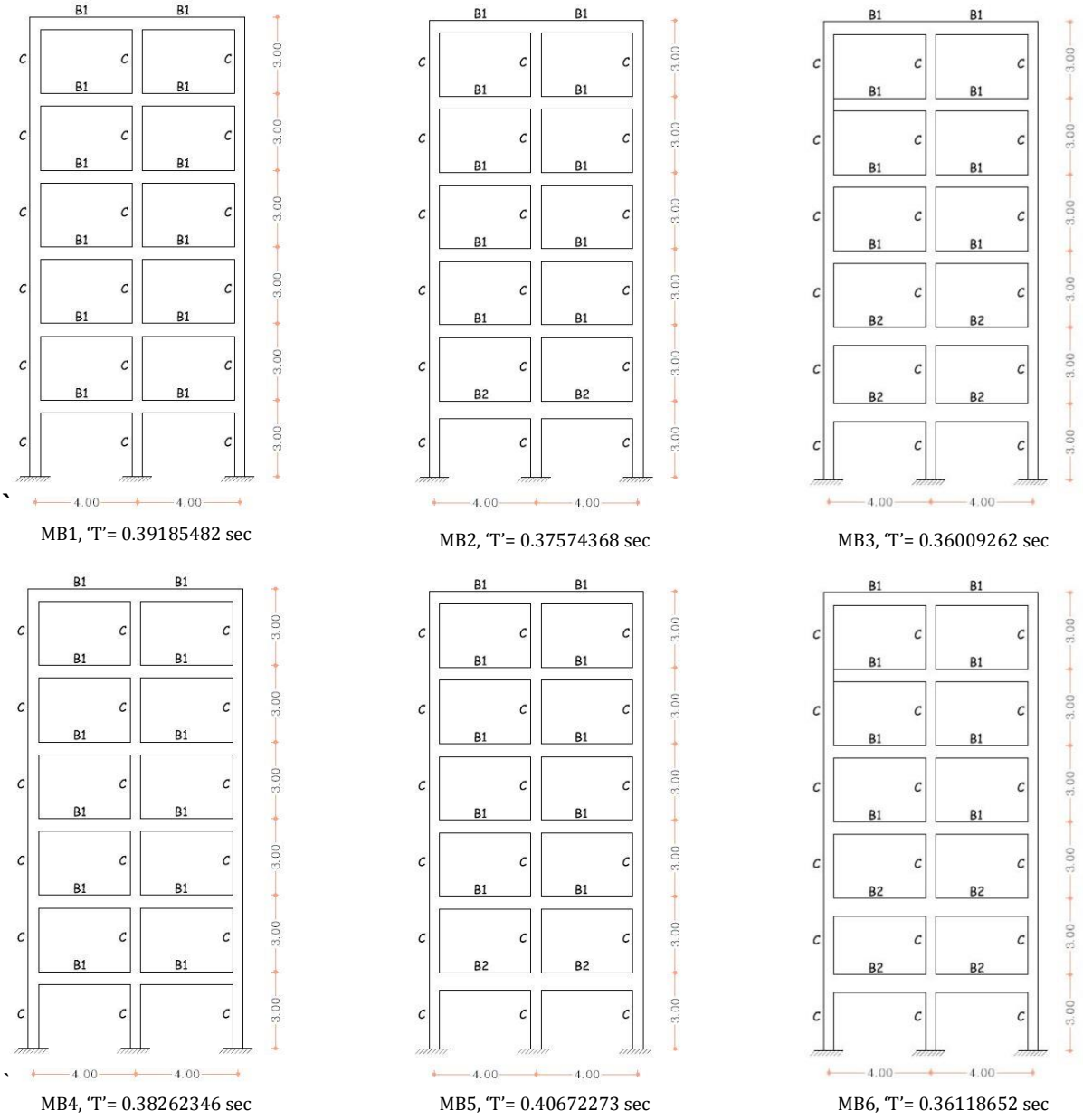

Fig. 3. Structural models for CASE 2-0 (elevation views)

3. Incremental Dynamic Analysis

To perform IDA, an appropriate set of ground motions is required. Several seismic codes (e.g. Uniform Building Code (UBC), 1997; Egyptian code for loads and ENV 1998-1, 2005) and researchers (e.g. Bommer et al., 2003) suggested a minimum of seven ground motions to be used to describe the behavior of a building under seismic loads. These ground motions can be selected from real records of earthquakes or can be generated artificially. Real records are more realistic since they include all ground motions characteristics such as amplitude, frequency, duration, energy content, number of cycles and phase (Rota et al., 2010). In this analysis, 10 records of ground motions were selected to perform the time history analysis of the chosen structures; all of them are real records of historical earthquakes. The characteristics of these ground motions are presented in Table 3.

During IDA, each ground motion was scaled incrementally up to 1.0g using a step of 0.2g. The maximum inter-storey drift ratio was calculated for each PGA, this represents a point on the IDA curve. The points of this drift ratio resulting from the various PGA values form the full IDA curve for a specific ground motion. The procedure was repeated for all 10 ground motions used in this paper. The full of fourteen IDA curves was extracted. Each curve characterizes the seismic response of a specific structural model under the effect of the ten ground motions. The IDA curves for the structural models are presented in Figs 4, 5 and 6 for CASE 1-1, CASE 1-2 and CASE 2-0 respectively.

The number of occurrence among the ground motions that exceeded certain performance level at each PGA value is calculated. Then the probability of exceeding this damage state was calculated. Mean and standard deviation, μ and σ, of the natural logarithm of PGA at

which each structure reaches the threshold of a specific damage state or performance level were calculated. These values are summered in Tables 4, 5 and 6 for CASE 1-1, CASE 1-2 and CASE 2-0 respectively, and were used in developing the fragility curves presented below.

As can be noted from all curves, IDA curve differs from one ground motion to another leading to a wide range of response for each structure. The common property shared by all curves is that data points create a linear region at lower scale factors. By increasing scale factor the curves begin to bend meaning that the structure begins to yield. For better assessment of structural performance, seismic fragility curves for each structure needs to be extracted at the five performance levels tabulated in Table 1.

The vertical gridlines on each curve at maximum inter-storey drift ratio of 0.005, 0.01, 0.015,0.02 and 0.025 represent performance level of OP, IO,DC, LS and CP respectively.

Table 3. Details of ground motions

No.	Ground motion	Station	Date	PGA (g)	Duration, Sec.
1	CHICHI	TAIWAN	Sep,20,1999	0.36	50
2	FRIULI	ITALY	May,06,1976	0.35	36
3	HOLLISTER	USA	Apr,09,1961	0.2	40
4	IMPERIAL VALLEY	USA	Oct,15,1979	0.32	40
5	KOBE	JAPAN	Jan,16,1995	0.34	40
6	KOCAELI	TURKEY	Aug,17,1999	0.35	35
7	LANDERS	USA	Jun,28,1992	0.64	48
8	LOMA, PRIETTA	USA	Oct,18,1989	0.36	40
9	NORTHRIDGE	USA	Jan,17,1994	0.57	40
10	TRNIDAD	USA	Aug,24,1983	0.19	21

4. Fragility Curves

Fragility curves are log-normal functions which express the probability of reaching or exceeding a specific damage state. They can be developed in terms of a seismic parameter, such as spectral acceleration, spectral displacement, peak ground velocity and PGA. Since PGA was the parameter used in developing the IDA in this work and also in previous researchers such as Ibrahim and El-Shami (2010), the PGA was selected to be the corresponding parameter in developing the fragility curves. The cumulative distribution functions was calculated by dividing the number of data points that reached or exceeded a particular damage state by the number of data points of the whole sample (Shinozuka et al., 2003). The conditional probability of a structure to reach or exceed a specific damage state, D, given the PGA, is defined by:

$$P\,[D/PGA] \;=\; \phi\,((\ln\,(PGA) - \mu)/\sigma))\,, \qquad (1)$$

where ϕ is the standard normal cumulative distribution function; μ and σ are the mean value and standard deviation of the natural logarithm of PGA at which the building reach the threshold of a specific damage state or performance level; D. Log-normal functions with two parameters (μ and σ) were fitted for different performance levels: OP, IO, DC, LS and CP, associated with the frames under study.

The input data points and the log-normal function fitted for different performance levels occurred in frame [SW1] (as an example) are shown in Table 7 and Fig. 7.

Referring to Table 7, it can be noticed that when frame SW1 is exposed to weak ground motion with PGA = 0.2g, the probabilities of exceeding the OP, IO, DC, LS and CP performance levels are 69%, 36%, 5% , 4% and 1% respectively. Also, the probability of exceeding a certain performance level increases by increasing PGA. Relations between PGA and probability for different performance levels of frame SW1 are plotted in Fig. 7 whereas Figs. 8, 9 and 10 represent the whole set of fragility curves for frames of CASE 1-1, CASE 1-2 and CASE 2-0 respectively.

It is obvious that in CASE 1-1, the probability of exceeding different performance levels for frame (SW1) is higher than its counterpart in (SW2) with a significant difference. This indicates that existence of exterior shear walls significantly enhances performance of the structure at different levels.

Interior shear walls (SW3) show slight improvement in performance of the structure compared to exterior shear walls (SW2).

Distributing shear walls externally and internally (SW4) gives an intermediate response between those for SW2 and SW3.

Generally, it is clear that different arrangements of shear walls along the strong direction of the structure have little effects on structural performance but the best performance was achieved when shear walls were accumulated internally. On the other hand, when earthquakes act on the weak direction of the structure (CASE 1-2), existence of exterior shear walls (SW6) slightly improves performance when compared to (SW5).

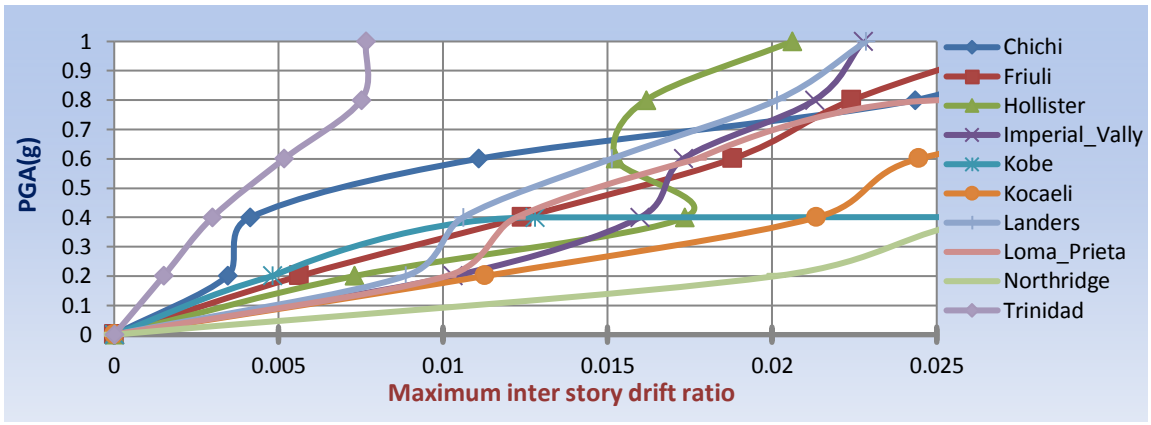

SW1

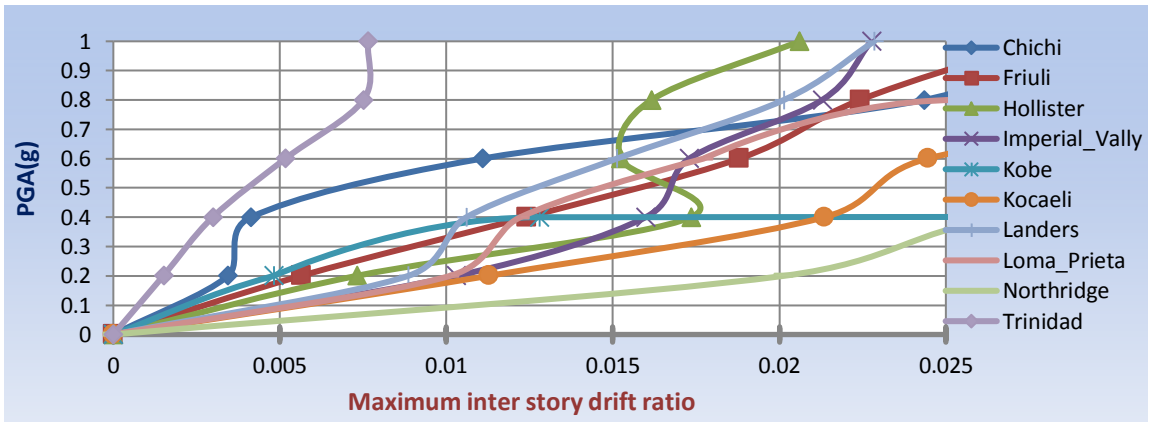

SW2

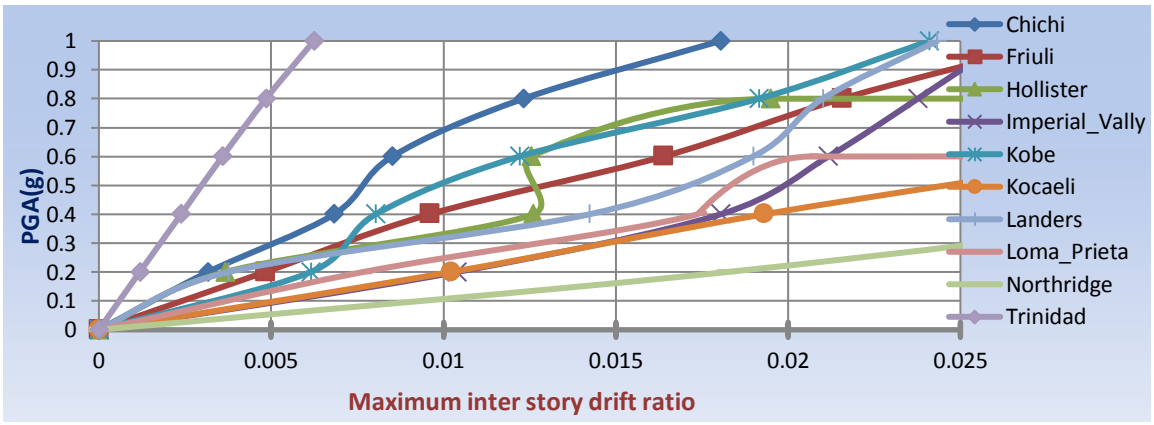

SW3

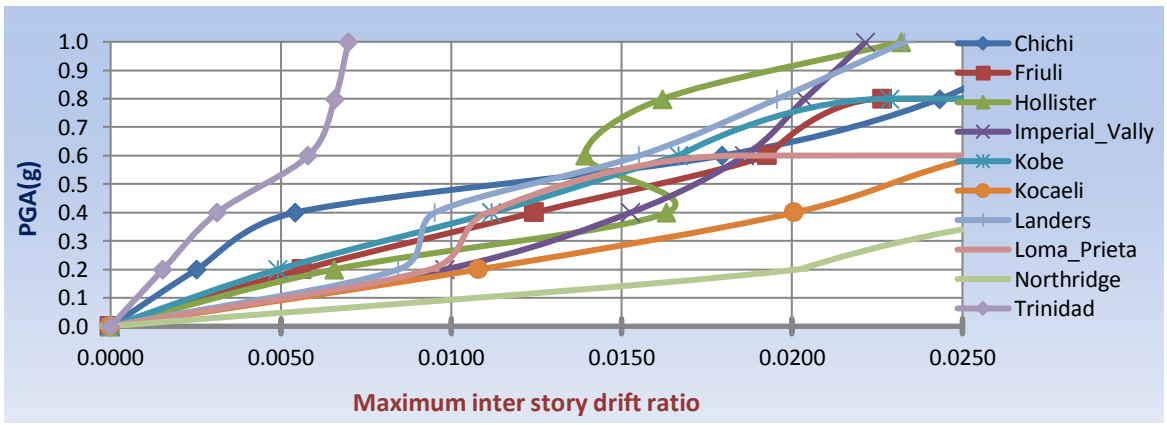

SW4

Fig. 4. Incremental dynamic analysis for the four frames in CASE 1-1.

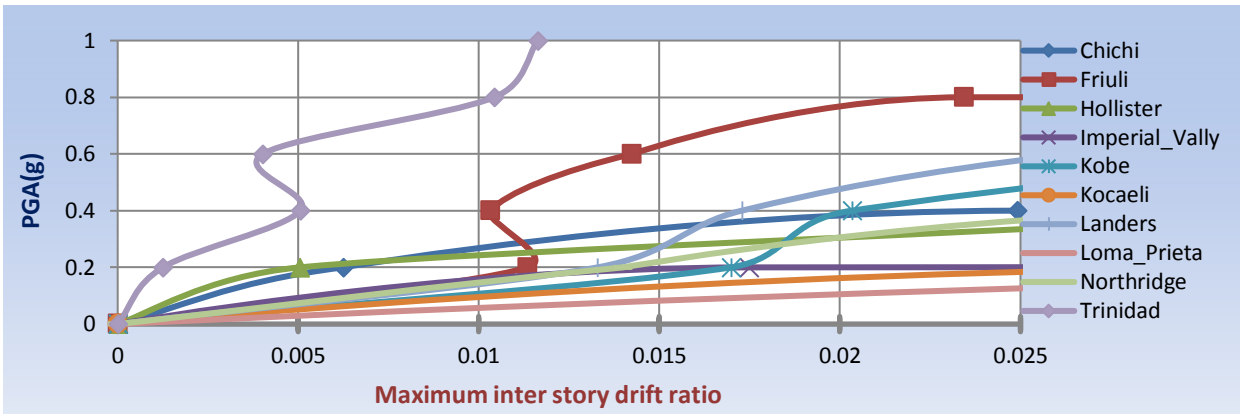

SW5

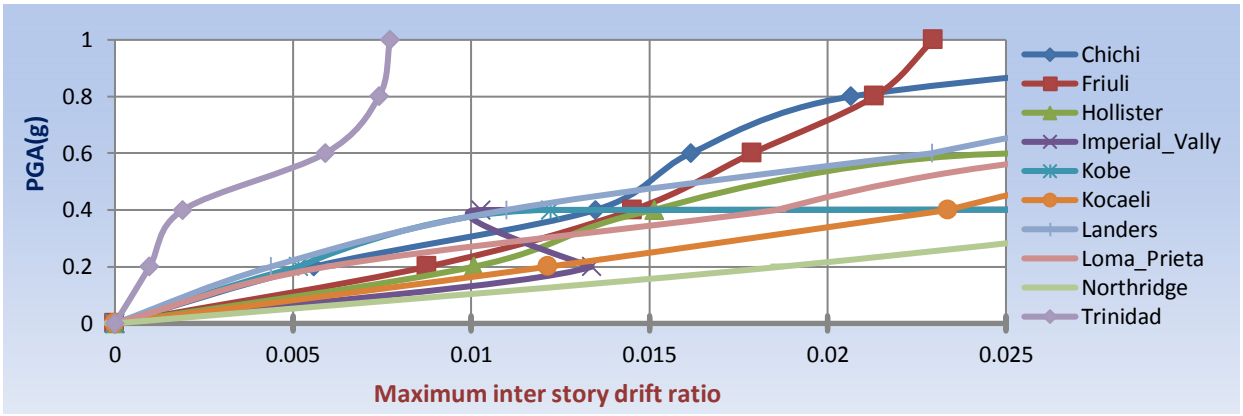

SW6

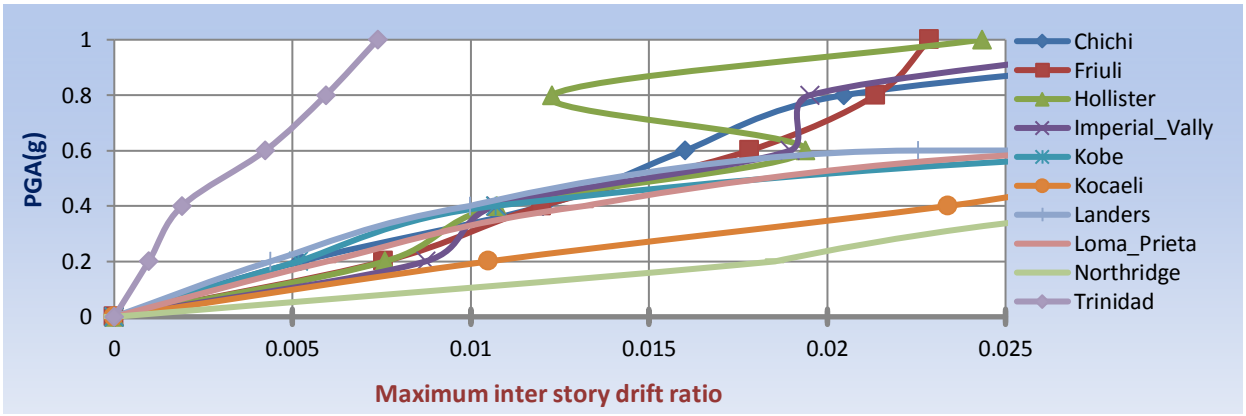

SW7

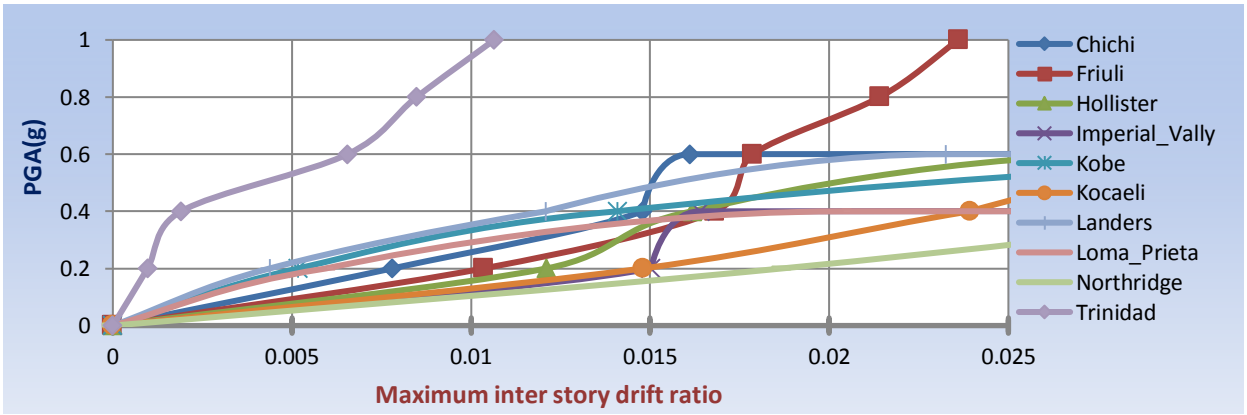

SW8

Fig. 5. Incremental dynamic analysis for the four frames in CASE 1-2.

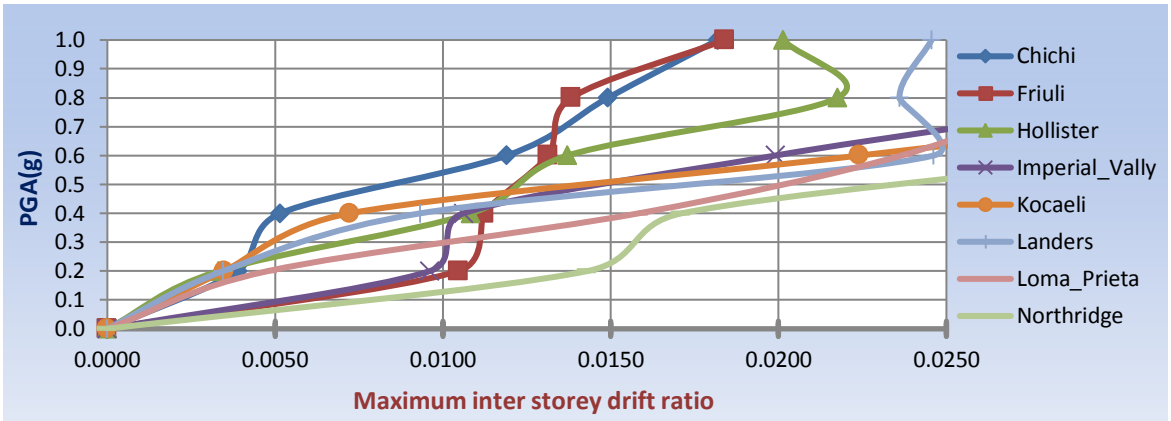

MB1

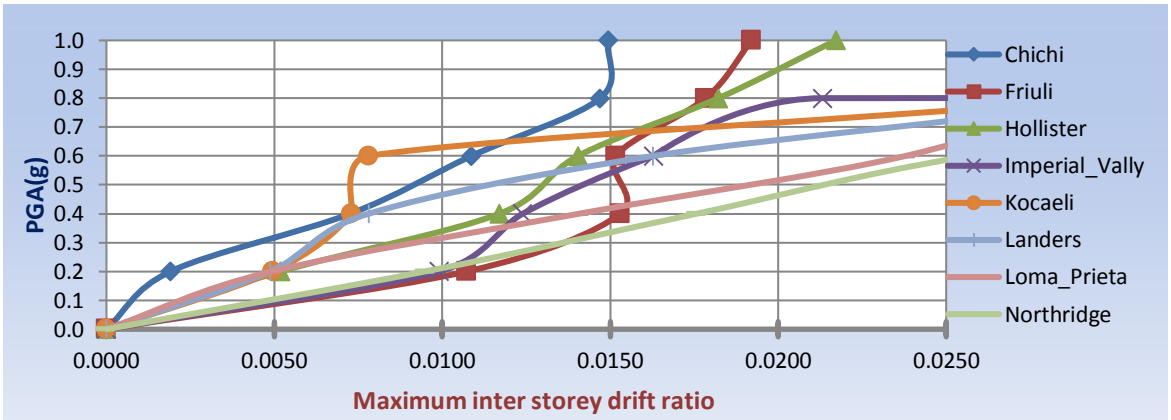

MB2

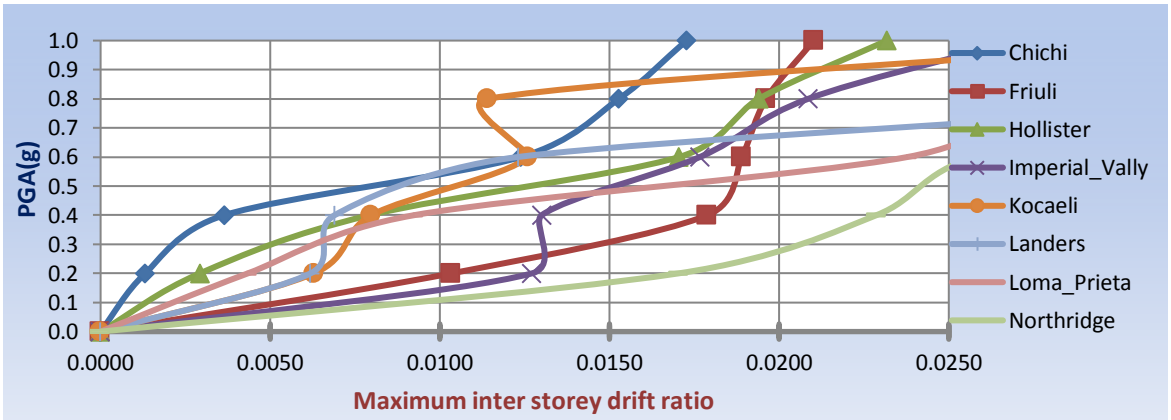

MB3

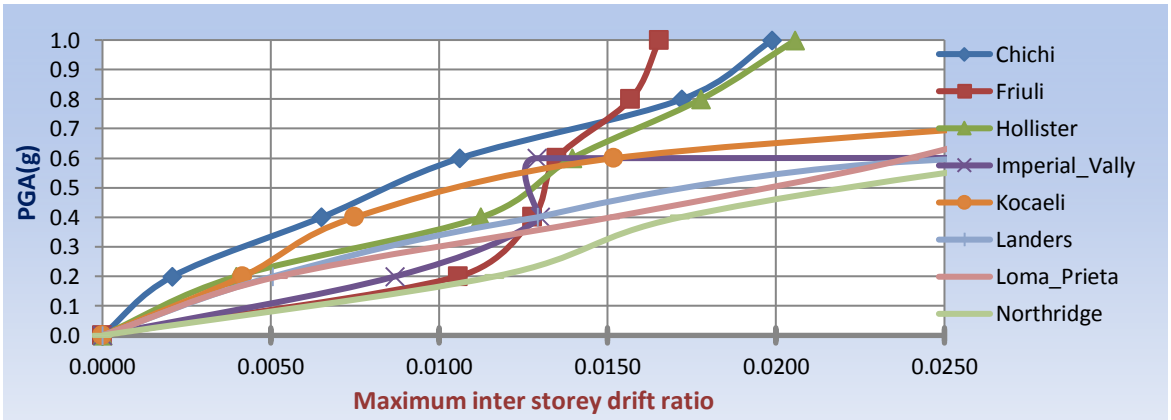

MB4

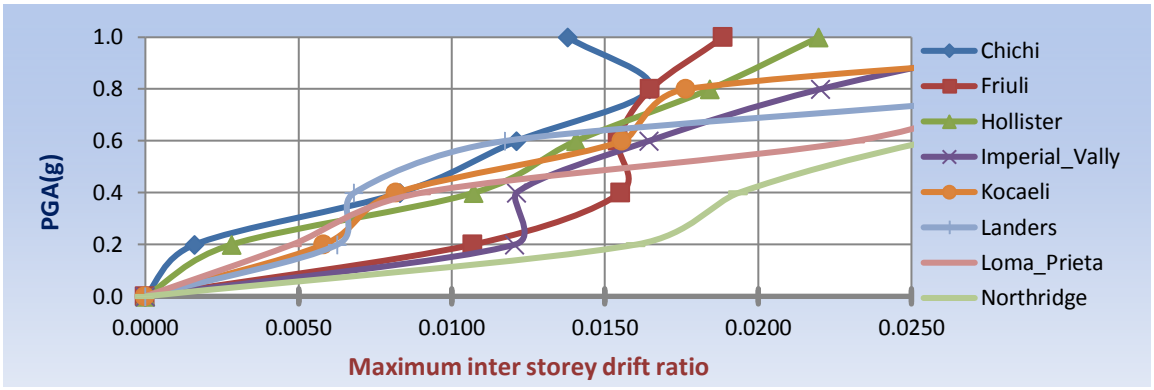

MB5

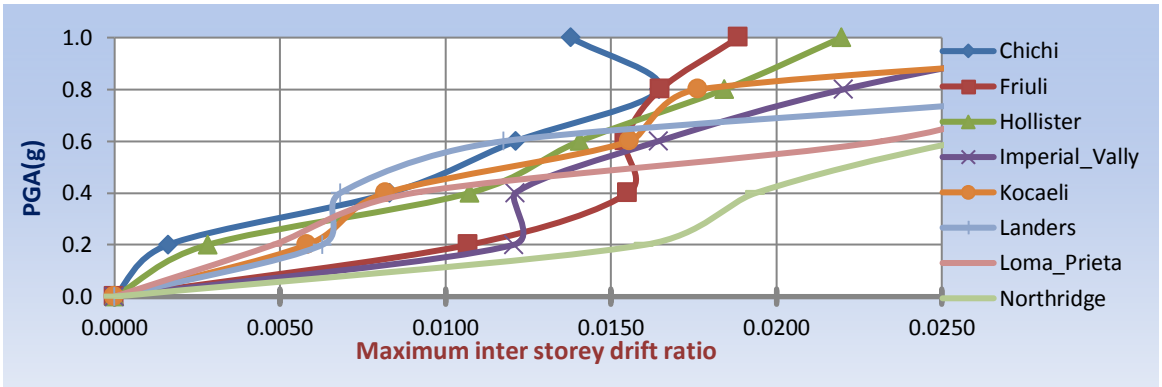

MB6

Fig. 6. Incremental dynamic analysis for the six frames in CASE 2-0.

Table 4. Parameters of log-normal distributions for fitting data for CASE 1-1 frames.

Frames	OP		IO		DC		LS		CP	
	μ	σ	μ	σ	μ	σ	μ	σ	μ	σ
SW1	0.128	0.925	0.259	0.726	0.438	0.477	0.494	0.505	0.596	0.470
SW2	0.108	0.900	0.237	0.878	0.410	0.535	0.562	0.567	0.825	0.580
SW3	0.150	0.855	0.297	0.801	0.447	0.630	0.628	0.628	0.914	0.656
SW4	0.108	0.900	0.273	0.786	0.430	0.513	0.637	0.578	0.896	0.544

Table 5. Parameters of log-normal distributions for fitting data for CASE 1-2 frames.

Frames	OP		IO		DC		LS		CP	
	μ	σ	μ	σ	μ	σ	μ	σ	μ	σ
SW5	0.069	0.824	0.142	0.786	0.212	0.943	0.286	0.821	0.309	0.861
SW6	0.119	0.789	0.223	0.860	0.370	0.613	0.455	0.547	0.550	0.467
SW7	0.223	0.549	0.270	0.748	0.431	0.511	0.594	0.449	0.714	0.517
SW8	0.093	0.909	0.209	0.902	0.337	0.651	0.437	0.541	0.529	0.500

Table 6. Parameters of log-normal distributions for fitting data for CASE 2-0 frames.

Frames	OP		IO		DC		LS		CP	
	μ	σ	μ	σ	μ	σ	μ	σ	μ	σ
MB1	0.146	0.579	0.234	0.522	0.443	0.420	0.610	0.441	0.734	0.417
MB2	0.116	0.416	0.294	0.525	0.493	0.275	0.726	0.359	0.818	0.289
MB3	0.137	0.582	0.277	0.599	0.438	0.454	0.693	0.482	0.842	0.334
MB4	0.123	0.477	0.287	0.398	0.486	0.282	0.668	0.382	0.734	0.417
MB5	0.137	0.582	0.278	0.383	0.423	0.374	0.578	0.439	0.684	0.490
MB6	0.123	0.477	0.260	0.567	0.445	0.373	0.728	0.428	0.842	0.334

Table 7. The probability of exceeding performance levels at certain PGA for frame [SW1].

PGA(g)	OP	IO	DC	LS	CP
0.0	0.00	0.00	0.00	0.00	0.00
0.1	0.39	0.09	0.00	0.00	0.00
0.2	0.69	0.36	0.05	0.04	0.01
0.3	0.82	0.58	0.21	0.16	0.07
0.4	0.89	0.72	0.42	0.34	0.20
0.5	0.93	0.82	0.61	0.51	0.35
0.6	0.95	0.88	0.74	0.65	0.51
0.7	0.97	0.91	0.84	0.76	0.63
0.8	0.98	0.94	0.90	0.83	0.73
0.9	0.98	0.96	0.93	0.88	0.81
1.0	0.99	0.97	0.96	0.92	0.86

The probability of exceeding the performance levels for frame (SW7) is lower than its counterpart in (SW6), this clarifies that existence of interior walls provides the structure with more efficiency than of exterior walls. In (SW8), the same number of walls was used but was distributed externally and internally. It was observed that the probability of reaching different performance levels in this case is higher than (SW7) and lower than (SW6). Based on the previously discussed results, it can be concluded that the best performance of the structure was reached in case of interior shear walls.

It is obvious that in CASE 2-0, the probability of exceeding the performance levels for the frame in the cases [MB1], [MB4] and [MB5] are higher than their counterparts in the case [MB2], [MB3] and [MB6], which means that existence of rigid marginal beam in lower levels gives more efficiency.

Lateral load resisting efficiencies in structure with rigid marginal beams in all floors and that for rigid marginal beam in the 1st floor are almost the same. This indicates that the existence of rigid marginal beam in the lower storey provides the best performance and the most economic situation.

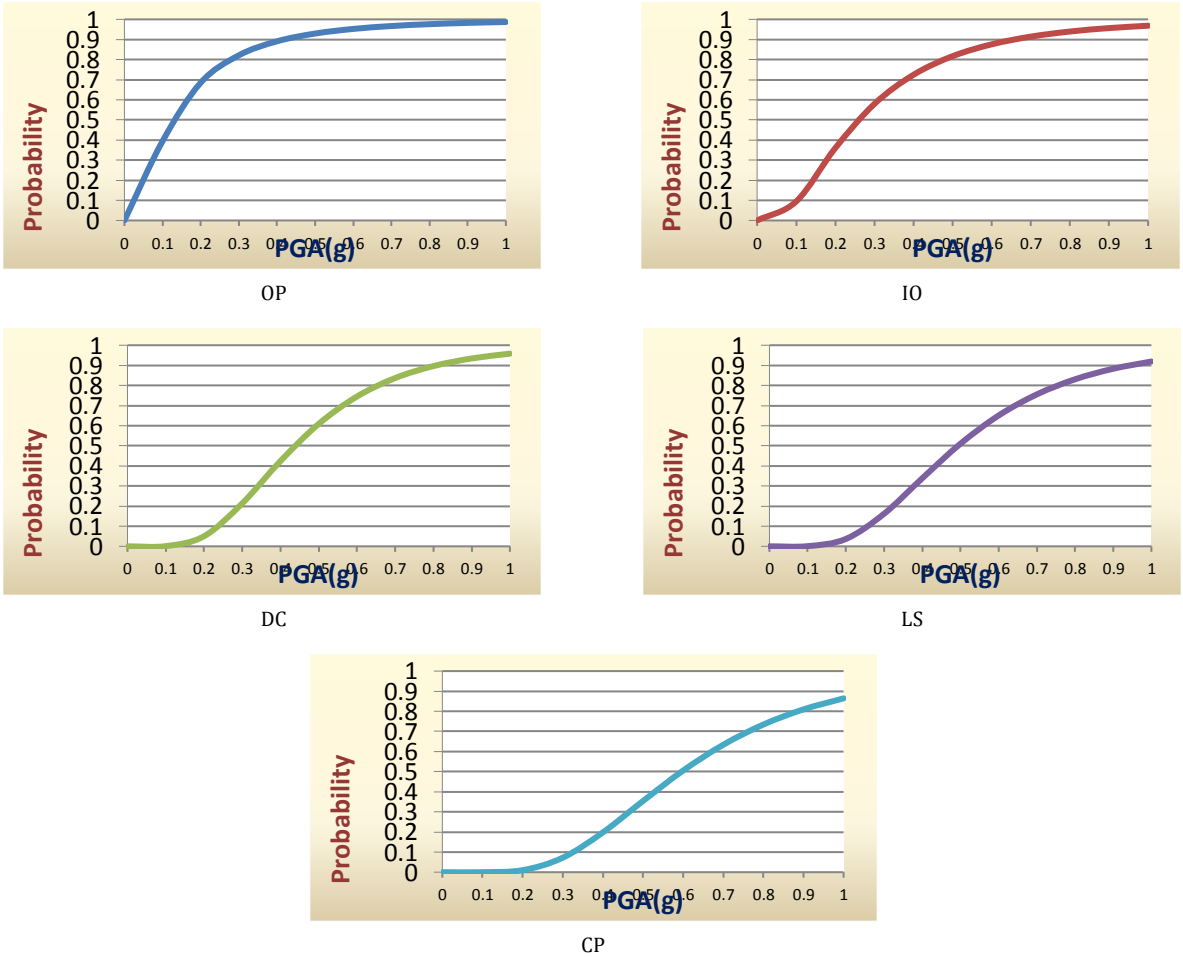

Fig. 7. Fitted curves for the frame SW1 at different performance levels.

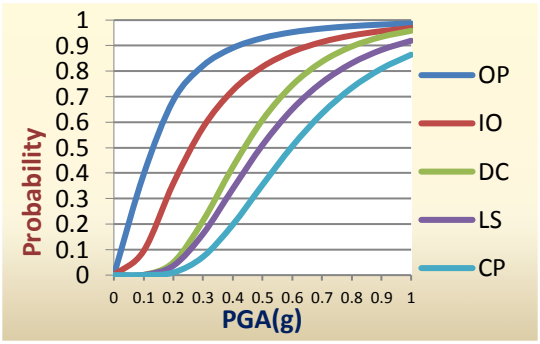

SW1

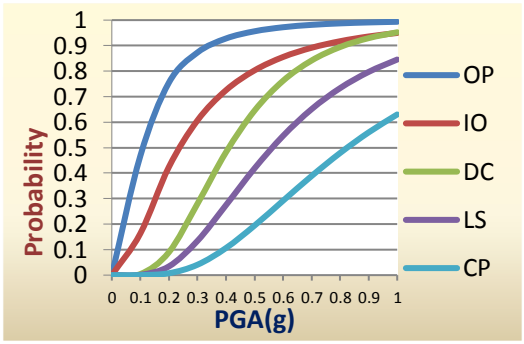

SW2

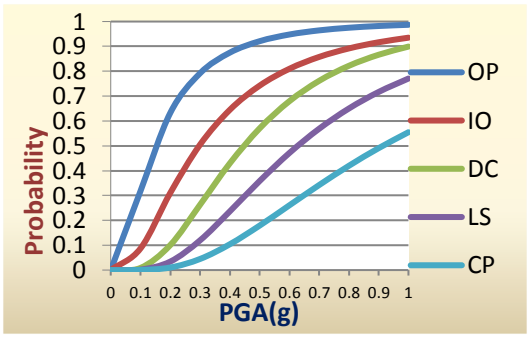

SW3

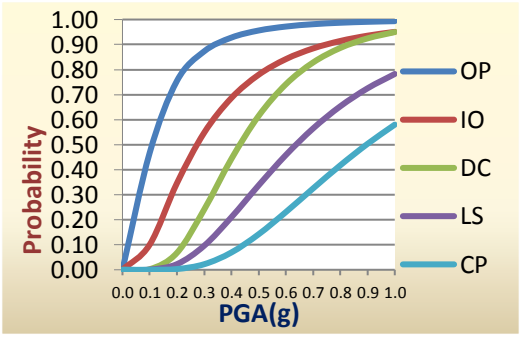

SW4

Fig. 8. Fragility curves for frames of CASE 1-1.

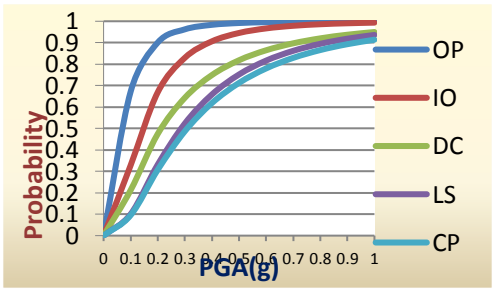

SW5

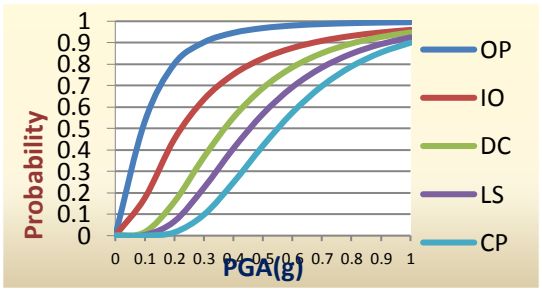

SW6

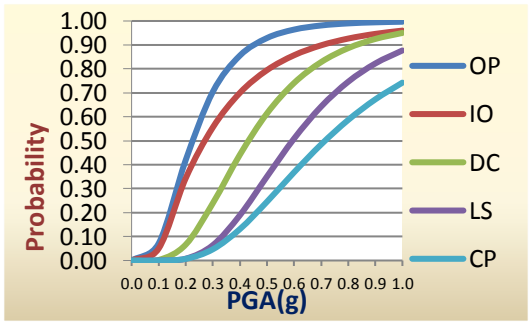

SW7

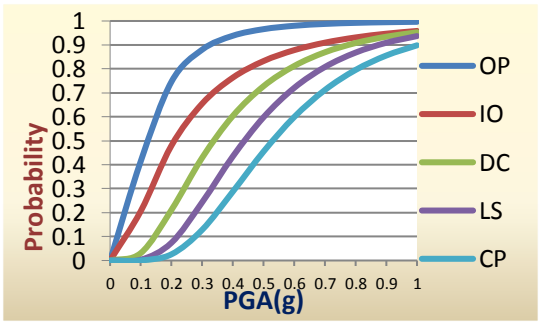

SW8

Fig. 9. Fragility curves for frames of CASE 1-2.

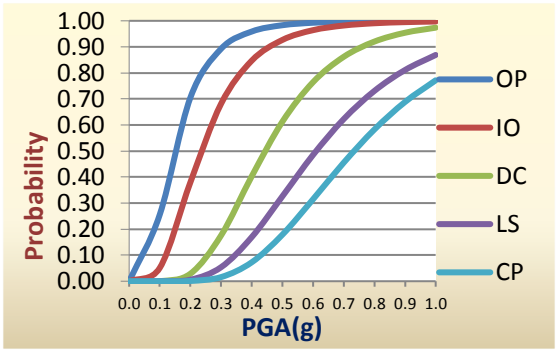

MB1

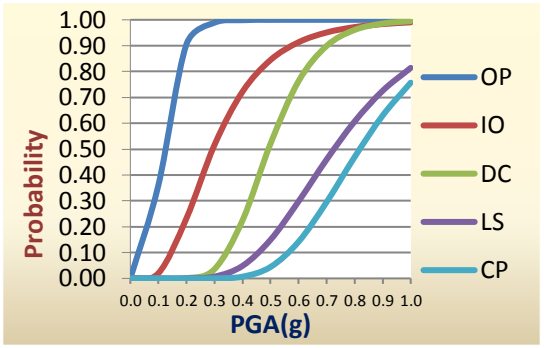

MB2

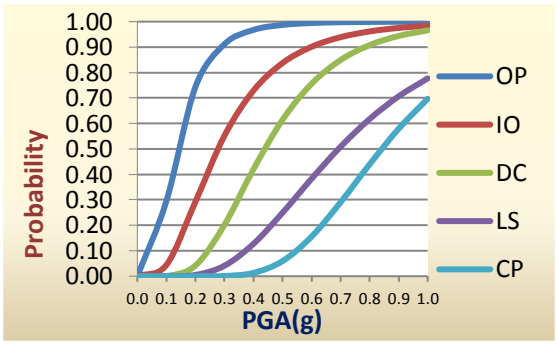

MB3

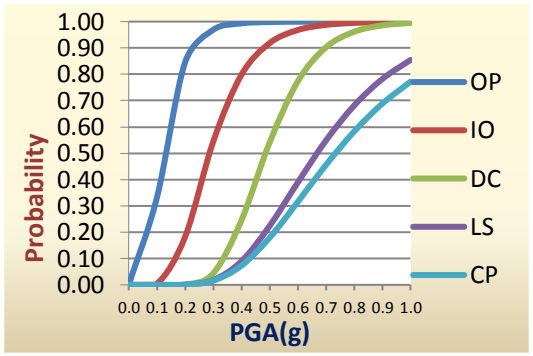

MB4

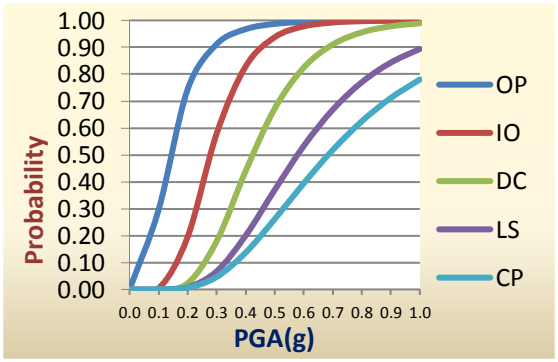

MB5

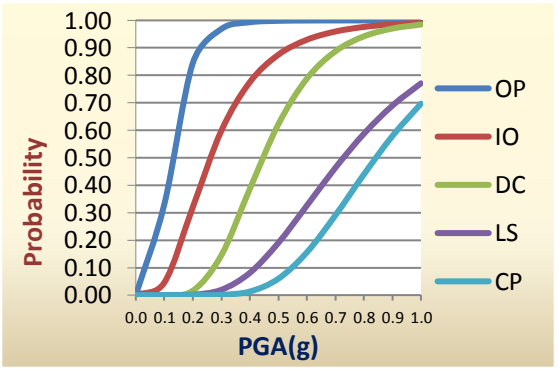

MB6

Fig. 10. Fragility curves for frames of CASE 2-0.

5. Conclusions

In this study, seismic fragility curves were conducted for R.C. 3D framed structures with different positions of shear walls as the first category of cases, two cases were considered CASE 1-1 and CASE 1-2 where in CASE 1-1, the structure was exposed to ground motions in its long direction while in CASE 1-2 ground motions act in the short direction. Ground motions were obtained from real records.

Also in this study, seismic fragility curves were conducted for R.C. 3D framed structures with different levels of the rigid marginal beam.

IDA was conducted using 'SeismoStruct' software under 10 ground motions. IDA curves showed wide range of behavior with large variation from record to record.

Different structural and non-structural performance levels were considered. These levels are operational (OP), immediate occupancy (IO), damage control (DC), life safety (LS) and collapse prevention (CP).

Based on the obtained results for different studied cases, it can be concluded that:

- Fragility curves are very useful tools for describing the behavior of certain structure under seismic loads. They also are considered as an excellent means of judgment and hence predicting the most efficient system for a certain structure.

- Different arrangements of shear walls in the structure produce different responses which lead to different performances.
- In frames of CASE1-1, shear walls, generally, play an important role in improving seismic performance of the structure, but no significant differences in performance were observed regarding to wall arrangement in the structure.
- In frames of CASE1-2, using interior shear walls gives the best behavior of the structure compared to exterior shear walls only and distributing shear walls internally and externally.
- The existing of rigid marginal beam in the lower storey shows the best structural resistance for lateral loads.

REFERENCES

ATC (2002). Development of Performance-Based Earthquake Design Guidelines. Redwood City: ATC-58.

Bommer JJ, Acevedo AB, and Douglas J (2003). The selection and scaling of real earthquake accelerograms for use in seismic design and assessment. In: Proceeding of ACI international conference on seismic bridge design and retrofit. La Jolla, CA: American Concrete Institute.

Cherng R (2001). Preliminary Study on the Fragility Curves for Steel Structures in Taipei. *Earthquake Engineering and Engineering Seismology*, 3(1), 35-42.

ECP 203 (2007). Egyptian code of practice for design and construction of concrete structures. National Center of Housing and Building Researches, Cairo, Egypt.

ENV 1998-1 (2005). Eurocode8: Design of Structures for Earthquake Resistance – Part 1: General rules, seismic actions and rules for buildings, Code of Practice, London.

Farsi M, Cherif F, Kaci S, Belaidi O, Taouche-Kheloui F (2015). Seismic vulnerability of reinforced concrete structures in Tizi-Ouzou City (Algeria). *1st International Conference on Structural Integrity*, 2015, 838-845.

Federal Emergency Management Agency (FEMA) 273 (1997). NEHRP guidelines for the seismic rehabilitation of buildings. Washington DC: Federal Emergency Management Agency.

Federal Emergency Management Agency (FEMA) 349, FEMA/EERI (2000). Action plan for performance – based seismic design. Washington DC: Federal Emergency Management Agency.

Federal Emergency Management Agency (FEMA) 356 (2000). Prestandard and commentary for the seismic rehabilitation of buildings. Washington DC: Federal Emergency Management Agency.

Federal Emergency Management Agency (FEMA) 450 (2003). NEHRP recommended provisions for seismic regulations for new buildings and other structures, Part 1: provisions. Washington DC: Federal Emergency Management Agency.

Hamburger RO (1998). Performance-based analysis and design procedure for moment resisting steel frames. Background Document, SAC Steel Project.

Heidebrecht A (2004). Code development issues arising from the preparation of the seismic provisions of the national building Code of Canada. 13WCEE, Vancouver, Canada: 3218-3228.

Ibrahim Y (2009). Performance limits of mid-rise moment-resisting framed structures in low seismicity areas. *11th Arab Structural Engineering Conference*, 25-27 October. Dhahran, Saudi Arabia: KFUPM.

Ibrahim Y and El-Shami M (2011). Seismic fragility curves for mid-rise reinforced concrete frames in Kingdom of Saudi Arabia. The IES Journal Part A: Civil & Structural Engineering, 4(4), 213-223

International Building Code (IBC) (2003). CA, USA: International Code Council, Delmar Cengage Learning.

Japan Structural Consultants Association (JSCA) (2000). Structural Design by Response Control Methods. Shoko-kusha Publishing Co. Ltd., Tokyo, Japan [in Japanese].

Khawar R, Yong-Sik C (2016). Building Damage Assessment Using Scenario Based Tsunami Numerical Analysis and Fragility Curves. Department of Civil and Environmental Engineering, Hanyang University, 222 Wangsimni-ro, Seongdong-gu, Seoul 04763, Korea; (CC-BY) license (http://creativecommons.org/licenses/by/4.0/).

King A, Shelton R (2004). New Zealand advances in performance-based seismic design. *13WCEE*, Vancouver, Canada: 13–25.

Kircil M, Polat Z (2006). Fragility analysis of mid-rise R/C frame buildings. *Engineering Structures*, 28(9), 1335-1345

Madas P (1993). Advanced Modeling of Composite Frames Subjected to Earthquake Loading. *Ph.D. Thesis,* London, UK: Imperial College, University of London.

Mander J, Dhakal R, Mashiko N, Solberg K (2007). Incremental dynamic analysis applied to seismic financial risk assessment of bridges. *Engineering Structures,* 29(10), 2662-2672.

Mander J, Priestley M, Park R (1988). Theoretical stress-strain model for confined concrete. *Journal of Structural Engineering,* 114(8), 1804-1826.

Moridani K, Khodayari R (2013). Seismic performance assessment uses incremental dynamic analysis. *Journal of Basic and Applied Scientific Research*, 3(8), 757-764.

Raipure P (2015). Seismic vulnerability assessment of open ground storey RC buildings by using fragility curves. *M-Tech Thesis*, Government College of Engineering, Amravati, 2013-14.

Rota M, Penna A, Magnes G (2010). A methodology for deriving analytical fragility curves for masonry buildings based on stochastic nonlinear analyses. Engineering Structures, 32, 1312-1323.

SeismoStruct Ver. 5.0.4, 2010. SeismoSoft, earthquake engineering software solutions [online]. Italy. Available from: www.seismosoft.com [Accessed 10 August 2011].

Shome N, Cornell CA (1999). Probabilistic Seismic Demand Analysis of Nonlinear Structures. *Ph.D. Thesis,* Stanford: Stanford University.

Structural Engineers Association of California, SEAOC, Vision 2000 (1995). Performance based seismic engineering of buildings. Sacramento, CA: Vision 2000 Committee.

Talaeitaba S, Tahvilian H, Saeedi B (2014). The effect of the arrangement and length of the concrete shear walls on the response modification factor (R). *Electronic Journal of Structural Engineering,* 14, 93-105.

Uriz P, Mahin S (2004). Seismic performance assessment of concentrically braced steel frames. *13th World Conference on Earthquake Engineering*, Vancouver, B.C., Canada

Vamvatsikos D, Cornell C.A (2002). Incremental dynamic analysis. *Journal of Earthquake Engineering and Structural Dynamics,* 31(3), 491-514.

Vazurkar U, Chaudhari D (2016). Development of fragility curves for RC buildings. *International Journal of Engineering Research,* 5(3), 591-594.

Xue Q, Wu CW, Chen CC, Chen KC (2008). The draft code for performance-based seismic design of buildings in Taiwan. *Engineering Structures*, 30(6), 1535–1547.

Challenge Journal of Concrete Research Letters

Comparative study of strengthening strategies for reinforced concrete frame with soft ground story

Md. Shafiqul Islam, Aojoy Shuvo *

Department of Civil Engineering, Rajshahi University of Engineering & Technology, 6402 Rajshahi, Bangladesh

ABSTRACT

One of the common forms of reinforced concrete (RC) framed building is to provide parking facility at ground level which is created by not providing any infill masonry at parking floor level. Due to the presence of infill walls in the entire upper story except for the ground story makes the upper stories much stiffer than the open ground story resulting in their poor performance during earthquakes. So strengthening of such reinforced concrete (RC) frame buildings with an open ground story is indispensable. In the present study several Strengthening options were evaluated for their effectiveness in improving the performance of such building without disturbing the parking facility of ground story based on linear and nonlinear analysis. The strengthening techniques studied were changing column dimension, providing diagonal bracing, lateral buttresses, shear wall, and providing chevron. The Strengthened building results were compared with the results of the original structure to deduce the structural performance improvement and cost associated to each solution were determined to develop cost efficiency relation for different strengthening technique. Providing lateral buttresses in the open first story was found to be more feasible in both case of increase ground story strength and economic point of view among all strengthening options.

ARTICLE INFO

Article history:
Received 17 October 2017
Accepted 29 November 2017

Keywords:
Reinforced concrete frame
Infill masonry
Strengthening options
Seismic effects
Cost–efficiency

1. Introduction

One of the common form of residential and commercial building in several countries is masonry-infilled reinforced concrete framed building with parking facility at ground level which is created by not providing any infill masonry at parking floor level .It introduces sudden discontinuities in the lateral strength and stiffness along its height .If the story stiffness is less than 70% of the floor immediately above it or less than 80% of the three floors above it, then the story is called soft story . The columns at such a floor, have a good possibility to get damaged to collapse under horizontal vibration due to earthquake. In considering the structural effect of infill in building design various national codes can be broadly grouped into two categories – those that consider the role of masonry infill (MI) wall while designing RC frames and those do not consider. A very few codes specifically recommend isolating the MI from the RC frames such that the stiffness of MI does not play any role on the overall stiffness of the frame (standards New Zealand NZS -3101, Russian SNIP -II -7-8D). Some national codes of a few countries: India-IS 1893(BIS 2002), Israel—SI 413 (SII 1995) and Bulgaria (Bulgarian Seismic Code 1987) recommend that the open-story beams and columns to be designed for higher forces obtained by multiplying the design seismic forces with predetermined factors varying from 2.1 to 3.0. In some past researches several strengthening techniques were recommended for open first story buildings. Sahoo and Rai (2013) recommend two techniques, first technique termed as column retrofit and the later technique termed as full retrofit. Kaushik et al. (2009) developed a rational method for the calculation of the required increase in strength of open – first story column. Furtado et al. (2015) studied four strengthening mechanisms,

* *Corresponding author*. E-mail address: aojoy.ce66@gmail.com (A. K. Shuvo)
ISSN: 2548-0928 / DOI: https://doi.org/10.20528/cjcrl.2017.04.003

namely: (a) RC column Jacketing, (b) introduction of RC shear wall, (c) introduction of steel bracing, (d) additional of steel bracing with energy dissipation device. This paper presents the analytical investigation of several strengthening mechanisms to improve the seismic performance of open first story RC frames. The parking facilities or other facilities for which the ground story was keep open were not be hampered by those strengthening mechanisms. All the strengthening strategies are applied to the outer side of building to make the ground story usable. Equivalent static analysis and nonlinear static analysis were carried out using ETABS 9.7.0.

2. Description of RC Building

For this study, 6-story building with twenty meter height, regular in plan was modeled. The building was fairly symmetric in plan and in elevation. The plan and elevation view of the building frame was studied as shown in Fig 1. In modeling plane frame the following material properties and geometrical properties was used for beam, columns, masonry infill. Columns were assumed to be fixed at the base. M-20 grade concrete and Fe-415 grade of reinforcing steel were used for all the frame models used in the study. Modulus of elasticity of concrete and masonry was 22361 MPa and 700 MPa respectively. Poison's ratio was 0.2 and 0.3 respectively for concrete and masonry. The unit weight of concrete and masonry was taken as 23.56 KN/m^3 and 20 KN/m^3. The floor finish and random wall on the floors were 1 KN/m^2. The live load on floor was taken as 2 KN/m^2. All beams and columns had cross sectional area e.g. 45cm X 30 cm and 45cm X 45 cm respectively. Infill walls and slabs were modeled as 20 cm and 15 cm thick respectively.

3. Masonry Infill in RC Structure

To understand the behavior of infilled frame many experimental and analytical research has been carried out in the past. Several analytical model has been developed for featuring infill characteristics in RC frame. Those models are mainly two categories: macro-model and micro model. Macro-model is based on equivalent strut method and most widely used for its simplicity. Thus masonry infilled RC frames can be modeled as equivalent braced frames with infill walls replaced by equivalent diagonal strut which can be used in nonlinear pushover analysis. The basic parameter of these struts is their equivalent width, which affects their stiffness and strength. Extensive research has been carried out to find out the width of equivalent strut, for example Holmes(1961), Stafford Smith and Carter (1969), Mainstone (1971), Paulay and Preistley (1992), Liauw and Kwan (1984), Hendry (1998). In the comparative study by K. H. Abdelkareem et al. (2013), of different expressions for the width of equivalent strut shows that the Paulay and Priestley equation is the most suitable, due to its simplicity and because it gives an approximate average value among those studied in that paper. Consequently, this method of modeling is being used in this study. The width of compressive struts is considered as one fourth of the diagonal length of the infill.

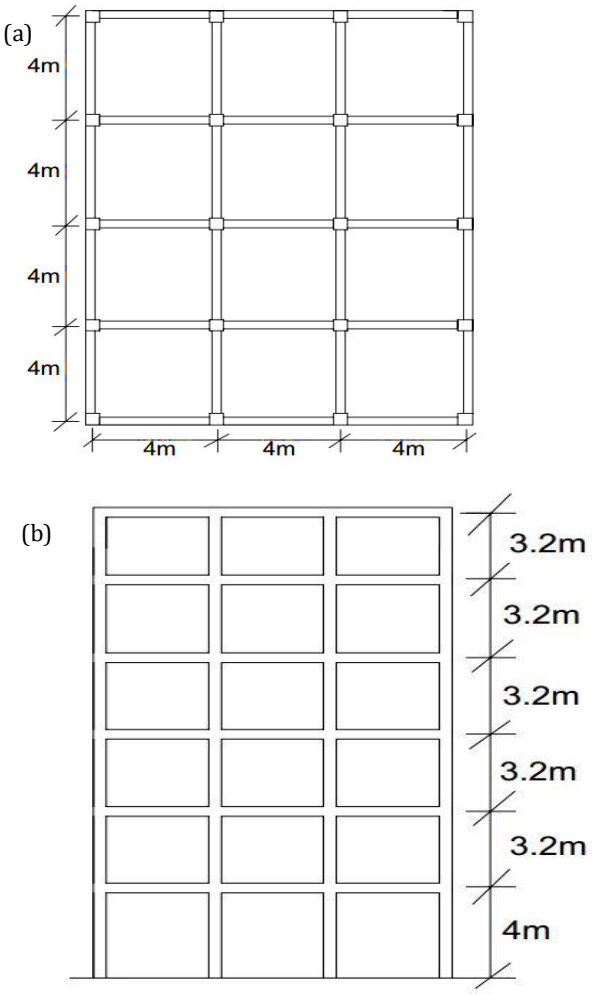

Fig. 1. General view of the building under analyses: (a) Building plan; (b) Building elevation.

4. Nonlinear Static Analysis

Nonlinear static analysis has become preferred analysis procedure for design and seismic performance evaluation purposes. It is an incremental static analysis used to determine the force displacement relationship. The most convenient way to plot the load deformation curve is by tracking the base shear and the roof displacement. The capacity of structure is represented by pushover curve. Pushover analysis was carried out for all the study frame to estimate seismic structural deformations. Default hinge properties were assigned to beams, columns and strut for pushover analysis. The built-in default hinge properties were typically based on FEMA-273 and ATC-40 criteria. Usually moment hinge properties (Default-M3) were assigned to beams and interacting hinge properties (Default-P-M-M) were assigned to columns and axial hinge properties (Default-P) were assigned to diagonal strut. The overall capacity of a structure depends on the strength and deformation capacities of the individual components of the structure. The building performance level can be determined by target displacement using the Capacity Spectrum method.

5. The Building Models Studied

Model 1 - This frame represents the most currently used common practice of not including the strength and stiffness of masonry infills in the analysis and design procedure. Effects of infills were not considered in all stories.

Model 2 - In this frame the effects of infills were considered in the upper stories; however, the first story of the frame was kept open.

Model 3 - In this frame for strengthening ground story, sectional area of all column of ground story increased by 1.5 times.

Model 4 - Diagonal bracings were provided in all external bays to improve lateral load performance of the frame. The size of section of bracings were same as to beam and plastic hinge properties of bracings were kept identical to that of the already existing first-story columns.

Model 5 - Lateral buttresses were provided in the open ground-story to ameliorate lateral strength. Inclination of buttresses with ground was 60^0. Sectional property and plastic hinge properties of the buttresses were kept identical to that of the columns in the first story.

Model 6 – In this frame shear walls were provided in ground story only in external four corner and wall thickness was provided as 25 cm.

Model 7 - Chevron were provided in all external bays. Sectional dimension was same as to beam and plastic hinge properties were kept identical to ground-story columns.

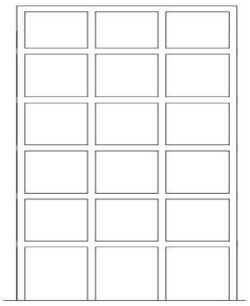

Fig. 2. Model 1

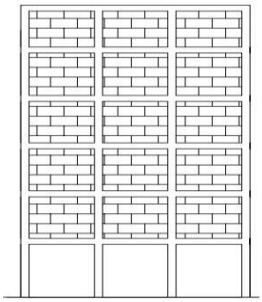

Fig. 3. Model 2

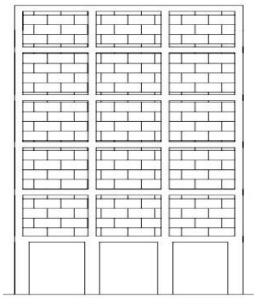

Fig. 4. Model 3

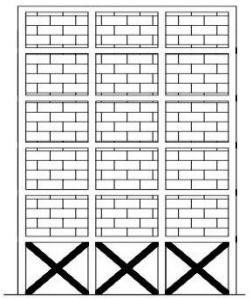

Fig. 5. Model 4

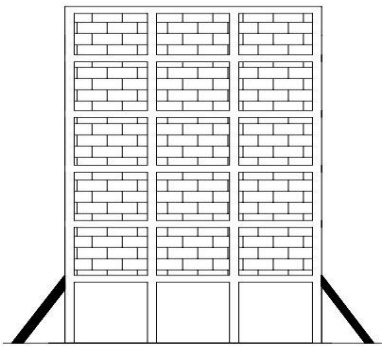

Fig. 6. Model 5

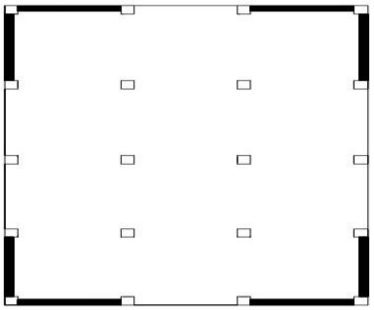

Fig. 7. Model 6 (Plan view)

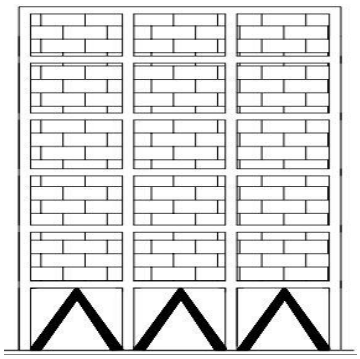

Fig. 8. Model 7

6. Results and Discussion

Linear and nonlinear analysis of different frames were carried out using ETABS software. The obtained results were represented graphically. Performance point of the building were obtained form of the results of pushover analysis.

6.1. Linear static analysis

Linear elastic analysis of the building were carried out using the equivalent static method. In the present investigation, earthquake load was chosen as a source of lateral loading on the building frame as set forth by the provision of Bangladesh National Building Code (BNBC, 1993). The total share force due to the seismic load was applied in the center of mass of all diaphragms with additional eccentricity ratio of all diaphragms. Earthquake load was applied at every story level of individual models. Drift pattern at different story level for different model are shown in Fig. 9.

6.2. Nonlinear static analysis

Pushover analysis were carried out for all the building models. First pushover analysis was done for the gravity loads (DL+0.25LL) incrementally under load control. The lateral pushover analysis was followed after the gravity pushover, under displacement control. The building was pushed in lateral directions until the formation of collapse mechanism. The capacity curve (base shear versus roof displacement) for different frames are presented in Figs. 10 and 11.

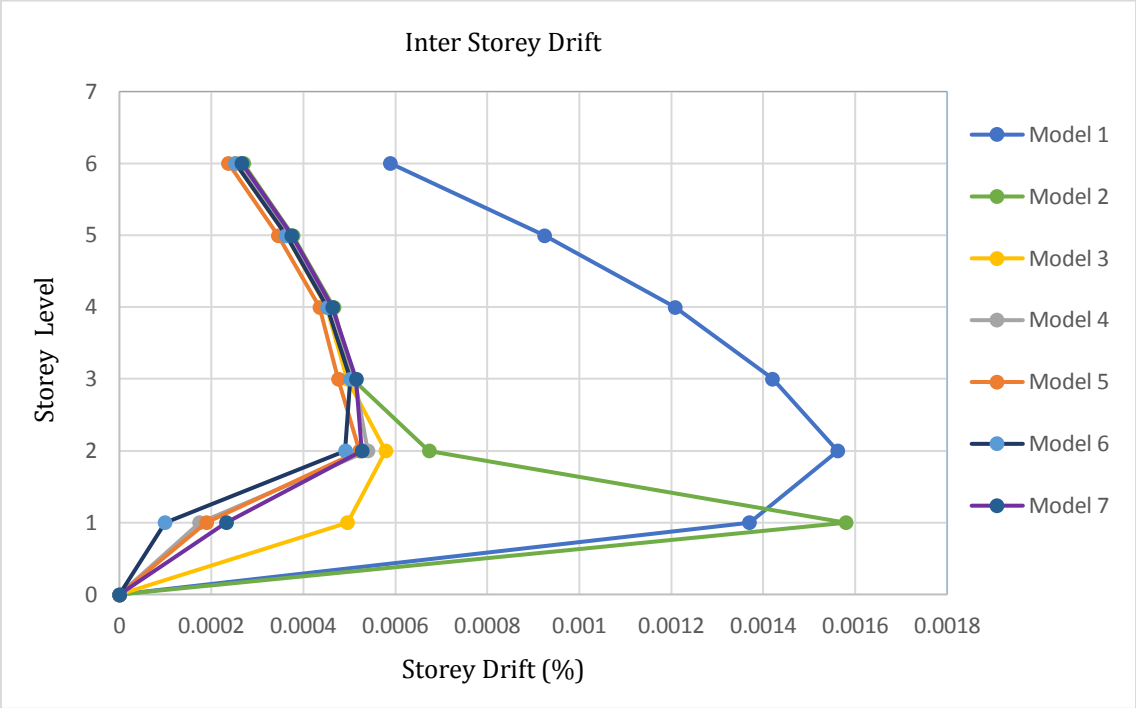

Fig. 9. Inter story drift of different model.

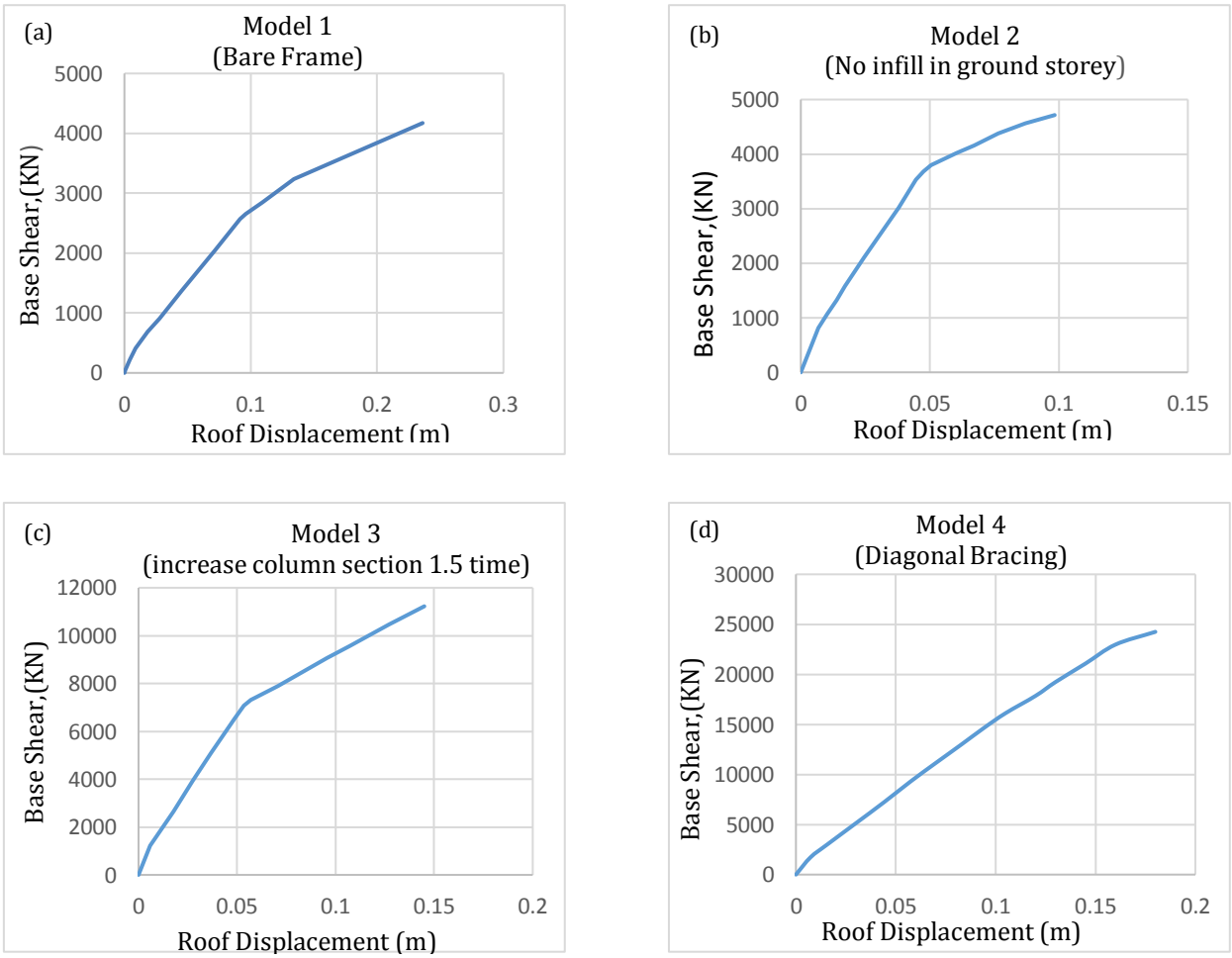

Fig. 10. Capacity curves:
(a) Model 1 (considering no infill); (b) Model 2 (no infill in ground story);
(c) Model 3 (increased column sectional area); (d) Model 4 (strengthened by x bracing).

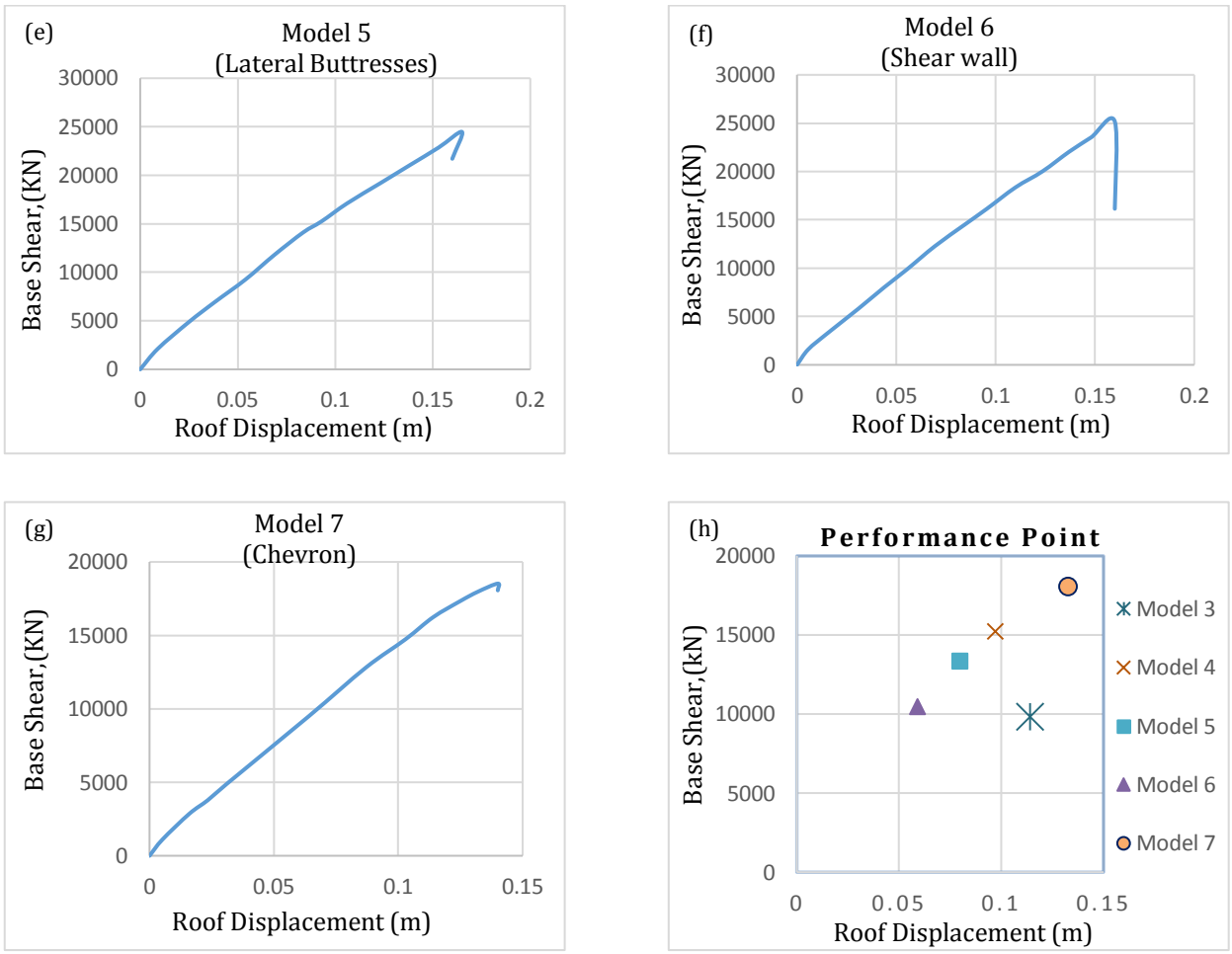

Fig. 11. Capacity curves:
(e) Model 5 (strengthened by lateral buttresses); (f) Model 6 (strengthened by shear wall);
(g) Model 7 (strengthened by chevron); (h) Performance point of different frame.

6.2.1. Performance points

Performance point obtained from pushover analysis shows the maximum structural displacement expected for the demand earthquake ground motion. The buildings were pushed to a displacement of 4% of height of the building to reach collapse point. Fig. 11(h) shows the comparison of the performance points obtained from pushover analysis of the different frames. Model 6(Shear Wall) exhibit minimum displacement and displacement for Model 4 and Model 5 is moderate, where in case of Model 7 high displacement occur. Model 3 exhibits displacement about 2 times of Model 6. The strengthening option Model 6 in which shear wall is provided in the open ground story, may be considered as the best strengthening solution. On the other hand, Model 5 in which additional lateral buttresses were provided in the open ground storey may be a good alternative for strengthening.

6.3. Cost–efficiency analysis

For cost efficiency comparison of each strengthening solution studied one indicator is used that would be take into account the value of the first-story maximum drift due to earthquake and the volume of concrete required for the strengthening solution (Fig. 12). The estimated volume of concrete for the strengthening solutions were taken as the percentage of volume required for beam, column and slab. It was observed that Model 3 (column section increased 1.5 times) exhibit maximum drift under earthquake but less cost among all solutions. Cost for Model 6 (shear wall) is maximum but it reduced about 93% drift of open ground story building. The cost and drift control performance of Model 4, Model 5 and Model 7 are moderate.

7. Conclusions

The seismic performance of RC frame with soft ground story was found to be very poor due to their inadequate lateral strength and drift control capacity. The effectiveness of the proposed strengthening techniques to improve the lateral load capacity of such buildings was evaluated by using pushover analyses. The strengthening schemes in which shear wall and lateral buttresses were provided in the open first story were found to be significantly more effective in improving both lateral strength and ductility of such frames. When diagonal

braces were used a huge increase in lateral strength and stiffness of the frame was observed. From cost-efficiency analysis providing lateral buttresses is most effective but if it will not convenient due to lack of space to provide buttresses then diagonal bracing or shear wall may be used.

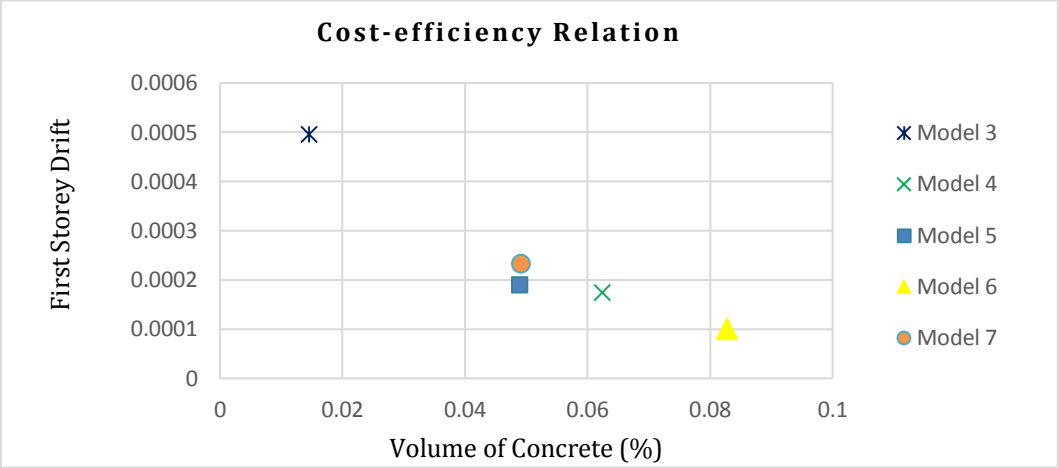

Fig. 12. Cost–efficiency comparison of strengthening solutions.

REFERENCES

Abdelkareem KH, Abdel Sayed FK, Ahmed MH, AL-Mekhlafy N (2013). Equivalent Strut Width for Modeling R.C. Infilled Frames. Civil Engineering Department, Faculty of Engineering, Assiut University.

Amin MR, Hasan P, Islam BKMA (2011). Effect of soft storey on multi storied reinforced concrete building frame. *4th Annual Paper Meet and 1st Civil Engineering Congress*, Dhaka, Bangladesh.

ATC (1996). Seismic Evaluation and Retrofit of Concrete Buildings. Applied Technology Council, Volume 1 (ATC-40), Report No. SSC 96-01. Redwood City (CA).

BIS (2002). Indian standard criteria for earthquake resistant design of structures. Bureau of Indian Standards, Part 1: General provisions and buildings. IS 1893, Fifth Revision, New Delhi, India.

BNBC (1993). Bangladesh National Building Code. Housing and Building Research Institute and Bangladesh Standards and Testing Institutions, Bangladesh.

Bulgarian Seismic Code (1987). Code for design of buildings and structures in seismic regions. Bulgarian Academy of Science Committee of Territorial and Town System at the Council of Ministers, Sofia, Bulgaria.

ETABS Nonlinear Version 9.7.0. Extended 3-D analysis of the Building Systems. California: Computers and Structures Inc. Berkeley.

FEMA 356 (2000). NEHRP Pre standard and commentary for the seismic rehabilitation of buildings. Federal Emergency Management Agency, Washington, D.C.

Furtado A, Rodrigues H, Varum H, Costa A (2014). Assessment and strengthening strategies of existing RC buildings with potential soft-storey response. *9th International Masonry Conference*, Guimaraes.

Furtado A, Rodrigues H, Varum H, Costa A (2015). Evaluation of different strengthening techniques' efficiency for a soft storey building. *European Journal of Environmental and Civil Engineering*, 21(4), 371-388.

Hendry AW (1998). Structural Masonry, 2nd ed. Macmillan Press, London.

Holmes M (1961). Steel frames with brick and concrete infilling. *Proceedings of Institution of Civil Engineers,* 19. 473-478.

Hoque KMAE (2006). A rationale for determining the natural period of RC building frames having infill. *Engineering Structures*, 28, 495–502.

Kasliwal NA, Rajguru RS (2016). Effect of numbers and positions of shear walls on seismic behaviour of multistoried structure. *International Journal of Science, Engineering and Technology Research*, 5(6), 2229-2232.

Kaushik HB, Rai DC, Jain SK (2009). Effectiveness of some strengthening options for masonry-infilled RC frames with open first story. *Journal of Structural Engineering*, 135(8), 925-937.

Liauw TC, Kwan KH (1984). Nonlinear behavior of non-integral infilled frames. *Computers & Structures*, 18, 551-560.

Narkhede DV, Deshkukh GP (2016). Performance of shear wall building at various positions by using pushover analysis. *International Journal of Research in Advent Technology,* Special Issue, 83-89.

NZS-3101(1995). Code of Practice for the Design of Concrete Structures. Part 1, Standards Association of New Zealand, Wellington, New Zealand.

Patel S (2012). Earthquake Resistant Design of Low-Rise Open Ground Storey Framed Building. *M.Sc. Thesis*, National Institute of Technology, Rourkela, India.

Pauley T, Priestley MJN (1992). Seismic design of reinforced and masonry buildings. Wiley Interscience Inc., USA.

Raju KL, Balaji KVGD (2015). Effective location of shear wall on performance of building frame subjected to earthquake load. *International Advanced Research Journal in Science, Engineering and Technology*, 2(1), 33-36.

Sahoo DR, Rai DC (2013). Design and evaluation of seismic strengthening techniques for reinforced concrete frames with soft ground story. *Engineering Structures*, 56, 1933-1944.

SII (1995). Design provisions for earthquake resistance of structures. Standards Institution of Israel, SI 413, Tel-Aviv, Israel.

Smith SB, Carter C (1969). A method of analysis for infilled frames. *Proceedings of Institution of Civil Engineers Part 2*, 44, 31-48.